ON OPTIMALLY SPARSE CYCLE AND COBOUNDARY BASIS FOR A LINEAR GRAPH

by

L. O. Chua and L. K. Chen

Memorandum No. ERL-M359

15 September 1972

ELECTRONICS RESEARCH LABORATORY

College of Engineering
University of California, Berkeley
94720

ON OPTIMALLY SPARSE CYCLE AND COBOUNDARY BASIS FOR A LINEAR GRAPH

by

L. O. Chua and L. K. Chen

Department of Electrical Engineering and Computer Sciences
and the Electronics Research Laboratory
University of California, Berkeley, California 94720

ABSTRACT

A graph-theoretic study of the computational efficiency of the generalized loop analysis and the generalized cut-set analysis is presented. It is shown that the choice of an optimum mode of analysis will give rise to the sparsest loop impedance matrix and the sparsest cut-set admittance matrix, respectively. The problem of formulating efficient algorithms for determining the optimum choice is shown to be strictly a problem in non-oriented linear graph. Two algorithms based on the concept of basis graph are presented and illustrated in details with examples. A non-planar version of the mesh analysis which generally yields a rather sparse loop impedance matrix is also included.

Research sponsored in part by the U. S. Naval Electronic Systems Command, Contract N00039-71-C-0255 and the National Science Foundation, Grant GK-32236.

I. INTRODUCTION

This paper is concerned with the computational efficiency of the two standard methods for formulating network equilibrium equations; namely, loop analysis, which includes mesh analysis as a special case, and cut-set analysis, which includes node analysis as a special case [1]. From the computer-aided analysis point of view, node analysis is preferred because it usually gives rise to a nodal admittance matrix $\underset{\sim}{Y}_n \triangleq \underset{\sim}{A}\underset{\sim}{G}\underset{\sim}{A}^T$ which is much sparser (i.e., contains less nonzero terms) than a corresponding cut-set admittance matrix $\underset{\sim}{Y}_q \triangleq \underset{\sim}{Q}\underset{\sim}{G}\underset{\sim}{Q}^T$ [2].[1] This observation is one of those "folk theorems" which has not been given a rigorous proof. In fact, as will be shown in the sequel, it is false that node analysis always gives rise to the sparsest cut-set admittance matrix; on the other hand, it is usually not worth the effort to try to find a cut-set admittance matrix which is sparser than the nodal admittance matrix. There would not be much point therefore in writing this paper if all networks can be analyzed via node analysis. Unfortunately, there exists a large class of networks which do not admit this mode of analysis. For example, networks containing nonlinear (non-monotonic) current-controlled resistors and/or dependent voltage sources require the loop analysis formulation.

The main motivation for this work is best illustrated by examining the nonlinear network shown in Fig. 1(a), where each nonlinear resistor R_i is characterized by a non-invertible function $v_i = R_i(j_i)$. Hence, node analysis is not possible for this network. The loop equations relative to the fundamental loop matrix $\underset{\sim}{B}$ in Fig. 1(b) is given by:

$$\left.\begin{aligned}
&R_1 o(j_1) - R_8 o(-j_1+j_2-j_3+j_4-j_5) - R_9 o(-j_1+j_2-j_3+j_4-j_5) = 0\\
&R_2 o(j_2) + R_8 o(-j_1+j_2-j_3+j_4-j_5) + R_9 o(-j_1+j_2-j_3+j_4-j_5) - R_{10} o(-j_2+j_3-j_4+j_5) = 0\\
&R_3 o(j_3) - R_8 o(-j_1+j_2-j_3+j_4-j_5) - R_9 o(-j_1+j_2-j_3+j_4-j_5) + R_{10} o(-j_2+j_3-j_4+j_5) = 0\\
&R_4 o(j_4) - R_7 o(-j_4+j_5) + R_8 o(-j_1+j_2-j_3+j_4-j_5) + R_9 o(-j_1+j_2-j_3+j_4-j_5) - R_{10} o(-j_2+j_3-j_4+j_5) = 0\\
&R_5 o(j_5) - R_6 o(-j_5) + R_7 o(-j_4+j_5) - R_8 o(-j_1+j_2-j_3+j_4-j_5) - R_9 o(-j_1+j_2-j_3+j_4-j_5)\\
&\qquad + R_{10} o(-j_2+j_3-j_4+j_5) = 0
\end{aligned}\right\} \quad (1)$$

where j_1, j_2, j_3, j_4, j_5 are the link currents and "o" denotes the composition operation. This system is strongly coupled in the sense that the argument of each function involves many variables. Had we chosen a different mode of loop analysis -- which in this planar network happens to be the mesh matrix $\underset{\sim}{M}$ in Fig. 1(c), the loop equations assume the greatly simplified form:

$$
\left.\begin{aligned}
&R_1 o(i_1+i_5) - R_8 o(-i_1) - R_9 o(-i_1) = 0\\
&R_2 o(i_2+i_5) + R_3 o(i_2+i_3) = 0\\
&R_3 o(i_2+i_3) + R_4 o(i_3+i_4) - R_7 o(-i_3) = 0\\
&R_4 o(i_3+i_4) + R_5 o(i_4) - R_6 o(-i_4) = 0\\
&R_1 o(i_1+i_5) + R_2 o(i_2+i_5) - R_{10} o(-i_5) = 0
\end{aligned}\right\} \quad (2)
$$

where i_1, i_2, i_3, i_4, i_5 are the mesh currents. These two systems of equations are equivalent in the sense that one can be derived from the other by elementary row operations. Yet (2) is so much simpler! The saving in computation may not be crucial for small linear networks; but for nonlinear networks where the Jacobian had to be evaluated numerically at each time step as in the Newton-Raphson iteration [2], or where the degree of coupling between terms is important in determining the existence and uniqueness of solution in a theoretical analysis [3 - 5], the advantage of (2) over (1) is indeed a decisive one — both from the computational and theoretical point of view. Consequently, this work is motivated mainly by the need for devising algorithms for formulating a system of equations of nonlinear networks having the least coupling among terms. The fact that these algorithms also lead to the sparsest (in the local optimal sense) loop impedance matrix $\underset{\sim}{Z}_\ell \triangleq \underset{\sim}{B}\underset{\sim}{R}\underset{\sim}{B}^T$ for linear networks provides yet another, although secondary, motivation.

A careful analysis of this problem shows that it involves only graph-theoretic concepts [6 - 10]. In fact, only the non-oriented graph is relevant. The basic definitions and terminologies are given in section II along with the formulation of a generalized method of loop analysis -- cycle analysis, and a generalized method of cut-set analysis -- coboundary analysis. In section III, the detailed vector space structure associated with these methods of analysis is developed and an exact formula for determining by inspection the "degree of coupling", or sparsity, of the associated matrices is derived. The concept of a basis graph is introduced as a useful aid toward the formulation of the desired algorithms. Two algorithms which provide a local optimal solution to the problem alluded earlier are presented in sections IV and V; they are called the nearest neighbor algorithm and the row-length minimization algorithm, respectively. Both of these algorithms are designed for large networks and are suitable for computer implementation. For smaller but non-planar networks, an algorithm is offered in section VI which can be interpreted as a pseudo-dual of node analysis. This algorithm can be implemented manually.

II. CYCLE AND COBOUNDARY ANALYSES

Consider the fundamental loop matrix $\underset{\sim}{B}$ of a connected oriented graph $\mathcal{G}$ having b branches and n nodes. It is well known that $\underset{\sim}{B}$ is a $\nu \times b$ matrix of entries -1, 0, and 1, where $\nu \triangleq b-n+1$, and that the row vectors of $\underset{\sim}{B}$ constitute a basis for a ν-dimensional vector subspace -- the cycle space $\mathcal{Z}(\mathcal{G})$ -- of $\mathbb{R}^b$ over the field $\mathbb{R}$ of real numbers. Each cycle basis (i.e., basis for the cycle space) $\mathcal{B}_{\mathcal{Z}}$ of $\mathcal{Z}(\mathcal{G})$ is therefore uniquely specified by a $\nu \times b$ matrix $\hat{\underset{\sim}{B}}$ -- henceforth called the cycle matrix. The fundamental loop matrix $\underset{\sim}{B}$ and the mesh matrix $\underset{\sim}{M}$ are only two of the many distinct cycle matrices.

It is also understood that relative to any cycle matrix $\hat{\underset{\sim}{B}}$, KVL takes the form $\hat{\underset{\sim}{B}}\underset{\sim}{v} = \underset{\sim}{0}$ and the cut-set transformation takes the form $\underset{\sim}{i} = \hat{\underset{\sim}{B}}^T\hat{\underset{\sim}{i}}$, where $\underset{\sim}{v}$ is the $b \times 1$ branch voltage vector, $\underset{\sim}{i}$ is the $b \times 1$ branch current vector, and $\hat{\underset{\sim}{i}}$ is a $\nu \times 1$ vector -- called the generalized current coordinates [6 - 8]. Hence, for a resistive network with a $b \times b$ branch resistance matrix $\underset{\sim}{R}$ and using the standard composite branch containing the sources as in [1], the network equilibrium equation takes the general form:

$$(\hat{\underset{\sim}{B}}\underset{\sim}{R}\hat{\underset{\sim}{B}}^T)\hat{\underset{\sim}{i}} = - \hat{\underset{\sim}{B}}\underset{\sim}{v}_s + \hat{\underset{\sim}{B}}\underset{\sim}{R}\underset{\sim}{j}_s \qquad (3)$$

We refer to (3) as the cycle analysis and the $\nu \times \nu$ matrix $\underset{\sim}{Z}_{\mathcal{Z}} \triangleq \hat{\underset{\sim}{B}}\underset{\sim}{R}\hat{\underset{\sim}{B}}^T$ as the cycle impedance matrix.[2] In the special case where $\hat{\underset{\sim}{B}}$ equals $\underset{\sim}{B}$ or $\underset{\sim}{M}$, $\underset{\sim}{Z}_{\mathcal{Z}}$ reduces to the loop impedance matrix $\underset{\sim}{Z}_{\ell}$ or mesh impedance matrix $\underset{\sim}{Z}_m$, and $\hat{\underset{\sim}{i}}$ reduces to the link current vector or mesh current vector, respectively.

For a nonlinear network containing current-controlled resistors, (3) assumes the form:

$$\hat{\underset{\sim}{B}}\underset{\sim}{R}^o(\hat{\underset{\sim}{B}}^T\hat{\underset{\sim}{i}}) = - \hat{\underset{\sim}{B}}\underset{\sim}{v}_s + \hat{\underset{\sim}{B}}\underset{\sim}{R}\underset{\sim}{j}_s \qquad (4)$$

where $R(\cdot)$: $\mathbb{R}^b \to \mathbb{R}^b$ denotes the b nonlinear functions. Since (3) and (4) are similar in form, it is clear that an algorithm which produces a sparser cycle impedance matrix $\underset{\sim}{Z}_{\mathcal{Z}}$ will also give rise to a weaklier coupled system of equations.

A dual development shows that the row vectors of a $\nu^* \times b$ fundamental cut-set matrix $\underset{\sim}{Q}$, where $\nu^* \triangleq n-1$, constitute a basis for the ν^*-dimensional coboundary space $\mathcal{Z}^*(\mathcal{G})$ [7 - 8]. Each coboundary basis $\mathcal{B}^*_{\mathcal{Z}^*}$ of $\mathcal{Z}^*(\mathcal{G})$ is uniquely defined by a $\nu^* \times b$ coboundary matrix $\hat{\underset{\sim}{Q}}$. The fundamental cut-set matrix $\underset{\sim}{Q}$ and the reduced incidence matrix $\underset{\sim}{A}$ are only two special cases of the coboundary matrices.

Corresponding to the cycle analysis (3), we now have:

$$(\hat{Q}G\hat{Q}^T)\,\hat{v} = -\hat{Q}j_s + \hat{Q}Gv_s \qquad (5)$$

where $\hat{v}$ is called the generalized voltage coordinates. We refer to (5) as the coboundary analysis and the $\nu^* \times \nu^*$ matrix $Y_{\partial^*} \triangleq \hat{Q}G\hat{Q}^T$ as the coboundary admittance matrix. In the special case where $\hat{Q}$ equals Q or A, Y_{∂^*} reduces to the cut-set admittance Y_q or the node admittance matrix Y_n, and $\hat{v}$ reduces to the tree-branch voltage vector or node-to-datum voltage vector, respectively.

We now see the cycle analysis as a generalized loop analysis and the coboundary analysis as a generalized cut-set analysis.[3] In either case, the problem is to devise algorithms for finding the sparsest cycle impedance (coboundary admittance) matrix Z_∂ (Y_{∂^*}).

It will be clear in the sequel that the orientation of the branches is irrelevant so far as constructing the algorithm is concerned. Consequently, throughout the remaining sections, only non-oriented graphs are considered and hence the cycle (coboundary) space needs only to be defined with respect to a mod 2 field.

III. THE CYCLE AND COBOUNDARY BASIS GRAPHS AND SPARSITY COEFFICIENTS

As a precise measure of the sparsity of $\hat{B}R\hat{B}^T$ and $\hat{Q}G\hat{Q}^T$, we define the following:

Definition 1. The cycle sparsity coefficient σ of a cycle impedance matrix $\hat{B}R\hat{B}^T$ is the number of nonzero terms in $\hat{B}R\hat{B}^T$.

Definition 2. The cycle matrix intersection coefficient, η_i, of row i of a cycle matrix $\hat{B}$ is the number of rows of $\hat{B}$ that have nonempty intersection with row i. Two rows $\hat{B}_i$ and $\hat{B}_j$ $(i \neq j)$, denoting the i^{th} and j^{th} row vectors of $\hat{B}$, are said to have nonempty intersection if there exists at least one k such that both column k of $\hat{B}_i$ and column k of $\hat{B}_j$ contain nonzero entries (i.e., $\hat{B}_i \cap \hat{B}_j \neq \emptyset$).

Definition 3. The cycle matrix nondiagonal intersection coefficient, μ_i, of row i of a cycle matrix $\hat{B}$ is the number of rows j, $j \neq i$, such that

(a) $\hat{B}_i \cap \hat{B}_j = \emptyset$;

(b) $(\hat{B}_i R) \cap \hat{B}_j \neq \emptyset$.

Definition 4. We define the coboundary sparsity coefficient σ^*, the coboundary matrix intersection coefficient η_i^*, and the coboundary matrix nondiagonal intersection coefficient μ_i^* to be the dual of those in Definitions 1 - 3.

Theorem 1. Let $\hat{Z}_\partial = \hat{B}R\hat{B}^T$ where $\hat{B}$ is a cycle matrix with dimension $\nu \triangleq b-n+1$ for a connected graph with b branches and n nodes, R is the $b \times b$ branch resistance

matrix which need not be symmetric, then

$$\sigma(\hat{\underset{\sim}{Z}}_{\mathcal{Z}}) = \nu + \sum_{i=1}^{\nu} \eta_i + \sum_{i=1}^{\nu} \mu_i \qquad (7)$$

Proof: The diagonal terms of $\hat{\underset{\sim}{Z}}_{\mathcal{Z}}$ are nonzero since

$$(\hat{\underset{\sim}{Z}}_{\mathcal{Z}})_{ii} = \sum_{k=1}^{b} (\hat{\underset{\sim}{B}}\underset{\sim}{R})_{ik}\hat{B}_{ik} = \sum_{k=1}^{b} \hat{B}_{ik}R_{kk}\hat{B}_{ik} = \sum_{k=1}^{b} (\hat{B}_{ik})^2 R_{kk} \neq 0,$$

for all i=1, 2, . . ., ν; otherwise $\hat{\underset{\sim}{B}}_i = \underset{\sim}{0}$ which can not be part of a basis. Let $i \neq j$, let $\underset{\sim}{R}^D$ be the matrix containing only the diagonal terms of $\underset{\sim}{R}$ and with the remaining entries zero, and let $\hat{\underset{\sim}{Z}}^D_{\mathcal{Z}} = \hat{\underset{\sim}{B}}\underset{\sim}{R}^D\hat{\underset{\sim}{B}}^T$, then

$$(\hat{\underset{\sim}{Z}}^D_{\mathcal{Z}})_{ij} = \sum_{k=1}^{b} (\hat{\underset{\sim}{B}}\underset{\sim}{R}^D)_{ik}\,\hat{B}_{jk} = \sum_{k=1}^{b} \hat{B}_{ik}\,\hat{B}_{jk}\,R^D_{kk} \neq 0 \Leftrightarrow \hat{\underset{\sim}{B}}_i \cap \hat{\underset{\sim}{B}}_j \neq \emptyset.$$

The number of nonzero elements of $\{(\hat{\underset{\sim}{Z}}^D_{\mathcal{Z}})_{ij}\} = \sum_{k=1}^{\nu} \eta_i$. Since $(\hat{\underset{\sim}{Z}}^D_{\mathcal{Z}})_{ij} \neq 0$ implies $(\hat{\underset{\sim}{Z}}_{\mathcal{Z}})_{ij} \neq 0$, the number of nonzero entries of $\hat{\underset{\sim}{Z}}_{\mathcal{Z}} \geq \nu + \sum_{i=1}^{\nu} \eta_i$. We know $(\hat{\underset{\sim}{Z}}^D_{\mathcal{Z}})_{ij} = 0$ $\Leftrightarrow$ $\hat{\underset{\sim}{B}}_i \cap \hat{\underset{\sim}{B}}_j = \emptyset$ and $(\hat{\underset{\sim}{Z}}_{\mathcal{Z}})_{ij} = \sum_{k=1}^{b} (\hat{\underset{\sim}{B}}\underset{\sim}{R})_{ik}\,B_{jk} \neq 0 \Leftrightarrow (\hat{\underset{\sim}{B}}\underset{\sim}{R})_i \cap \hat{\underset{\sim}{B}}_j \neq \emptyset$, therefore, the number of nonzero entries of $\hat{\underset{\sim}{Z}}_{\mathcal{Z}}$ that has corresponding zero entry in $\hat{\underset{\sim}{Z}}^D_{\mathcal{Z}}$ is equal to $\sum_{i=1}^{\nu} \mu_i$. It is obvious, then, (7) holds. ¤

If we define the cycle matrix intersection coefficient slightly differently as:

Definition 5. The cycle matrix intersection coefficient, σ_i, of row i of a cycle matrix $\hat{\underset{\sim}{B}}$ is the number of row j such that

(a) $j \in \{i+1, i+2, \ldots, \nu\}$;

(b) $\hat{\underset{\sim}{B}}_i \cap \hat{\underset{\sim}{B}}_j \neq \emptyset$.

Then some immediate consequences from Theorem 1 can be stated as follows:

Corollary 1. $$\sigma(\hat{\underset{\sim}{Z}}_{\mathcal{Z}}) = \nu + 2\sum_{i=1}^{\nu-1} \sigma_i + \sum_{i=1}^{\nu} \mu_i \qquad (8)$$

Corollary 2. If $\underset{\sim}{R}$ is diagonal, then

$$\sigma(\hat{\underset{\sim}{Z}}_{\mathcal{Z}}) = \nu + 2\sum_{i=1}^{\nu-1} \sigma_i \qquad (9)$$

The above theorem defines a mapping between any cycle matrix and the number of nonzero terms of its corresponding cycle impedance matrix. The part "ν" in (8) can not be minimized; we can only try to minimize the part "$2\sum_{i=1}^{\nu-1} \sigma_i + \sum_{i=1}^{\nu} \mu_i$."

In general, $\sum_{i=1}^{\nu} \mu_i << 2 \sum_{i=1}^{\nu-1} \sigma_i$, and because μ_i is much harder to find by inspection than σ_i (see Appendix A), we shall ignore $\sum_{i=1}^{\nu} \mu_i$ and work only on minimizing $2 \sum_{i=1}^{\nu-1} \sigma_i$. In other words, we assume $\underset{\sim}{R}$ to be diagonal. By this assumption, we can make our algorithms much more efficient.

Before introducing the concept of basis graph, we need another theorem:

Theorem 2. For a cycle space $\mathcal{Z}(\mathcal{G})$ of dimension $\nu \triangleq b-n+1$, there are exactly $N_\nu \triangleq \frac{1}{\nu!} \prod_{i=0}^{\nu-1} (2^\nu - 2^i)$ distinct cycle bases.

Proof: Since there are ν elements in the basis and the vector space is modulo 2, by either take or not take each element in the given basis, we come up with $2^\nu-1$ nonzero element in $\mathcal{Z}(\mathcal{G})$. The number of choices for the first element of a basis can be any one of the $2^\nu-1$ nonzero terms. The number of choices for the second element of a basis is restricted in the sense that it has to be independent on the first element. In other words, the second element can be any nonzero element outside the subspace generated by the first element. Therefore, the number of choices for the second element of a basis is $(2^\nu-1)-(2^1-1) = 2^\nu-2^1$. Similarly, the number of choices for the third element of a basis is $(2^\nu-1)-(2^2-1) = 2^\nu-2^2$, . . ., the number of choices for the νth element of a basis is $2^\nu-2^{\nu-1}$. The total number of choices is $(2^\nu-1)(2^\nu-2^1)(2^\nu-2^2) \ldots (2^\nu-2^{\nu-1}) = \prod_{i=0}^{\nu-1} (2^\nu-2^i)$. Since there is a redundancy of $\nu!$ for choosing bases, the number of distinct cycle basis is $\frac{1}{\nu!} \prod_{i=0}^{\nu-1} (2^\nu-2^i)$. ¤

Since the number of distinct cycle bases (or cycle matrices) in $\mathcal{Z}(\mathcal{G})$ is finite, there exists a cycle matrix with its corresponding impedance matrix having the smallest σ value, σ_{opt}, denoted as $\hat{\underset{\sim}{B}}_{opt}$. The flow chart for generating all N_ν distinct cycle bases without duplication and for finding σ_{opt} is given in Appendix B. An exhaustive search over all cycle matrices will obviously yield the optimum cycle matrix $\hat{\underset{\sim}{B}}_{opt}$. However, this is clearly impractical except for very small networks, say $\nu < 5$. This motivates the search for more efficient algorithms.

Definition 6. A cycle basis graph $\mathcal{GB}_{\mathcal{Z}}$ of a cycle space $\mathcal{Z}(\mathcal{G})$ is a graph with each node corresponding to a distinct cycle basis (or cycle matrix) of $\mathcal{Z}(\mathcal{G})$ and and a branch connecting nodes $\hat{\underset{\sim}{B}}$ and $\hat{\underset{\sim}{B}}'$ ⇔

(a) $\exists$ one and only one k such that $\hat{\underset{\sim}{B}}_k = \hat{\underset{\sim}{B}}'_k + \hat{\underset{\sim}{B}}'_\ell$ where $\ell \neq k$,

(b) $\forall\ \ell \neq k$, $\hat{\underset{\sim}{B}}_\ell = \hat{\underset{\sim}{B}}'_\ell$.

Definition 7. Nodes $\hat{\underset{\sim}{B}}$ and $\hat{\underset{\sim}{B}}'$ are said to be neighbors to each other iff they are connected by a branch in the cycle basis graph $\mathcal{G}_{\mathcal{B}_\mathcal{Z}}$.

Observe that in the cycle basis graph $\mathcal{G}_{\mathcal{B}_\mathcal{Z}}$ of a cycle space $\mathcal{Z}(\mathcal{G})$ with dimension ν, each node has exactly $\nu(\nu-1)$ neighbors. This observation will be used in the algorithm to be presented in the next section.

From duality, we have

$$\sigma^*(\hat{\underset{\sim}{Y}}_{\mathcal{Z}^*}) = \nu^* + 2\sum_{i=1}^{\nu^*-1} \sigma_i^* + \sum_{i=1}^{\nu^*} \mu_i^* \tag{9}$$

and the coboundary basis graph $\mathcal{G}_{\mathcal{B}_{\mathcal{Z}^*}}$ is defined accordingly.

An example is given next to illustrate (8) and (9). Consider the circuit shown in Fig. 2(a), and assume no dependent sources or coupling elements. Let $\underset{\sim}{B}$ be the fundamental loop matrix with respect to the tree {11, 12, . . ., 21}, $\underset{\sim}{M}$ be the mesh matrix, $\underset{\sim}{Q}$ be the fundamental cutset matrix with respect to the tree {11, 12, . . ., 21}, $\underset{\sim}{A}$ be the reduced incidence matrix, and $\hat{\underset{\sim}{Q}}$ be a coboundary matrix. $\underset{\sim}{B}$, $\underset{\sim}{M}$, $\underset{\sim}{Q}$, $\underset{\sim}{A}$, $\hat{\underset{\sim}{Q}}$ are represented in Figs. 2(b), (c), (d), (e), (f), respectively.

Consider Fig. 2(b), the "x" denotes the nonzero term while the zero terms are left blank. The rightmost column contains the cycle matrix intersection coefficient σ_i. Since $\underset{\sim}{B}_1$ intersects $\underset{\sim}{B}_2$ (at columns 17 and 18), $\underset{\sim}{B}_3$ (at columns 17 and 18), $\underset{\sim}{B}_4$, and $\underset{\sim}{B}_5$, $\sigma_1 = 4$ as shown in the first row of the rightmost column. $\underset{\sim}{B}_2$ intersects $\underset{\sim}{B}_3$ (at columns 17, 18, and 19), $\underset{\sim}{B}_4$, and $\underset{\sim}{B}_5$, therefore, $\sigma_2 = 3$. And in the last row of the rightmost column we have the value of $\sum_{i=1}^{\nu-1} \sigma_i$ as abbreviated by "$\sum$". For the fundamental loop matrix $\underset{\sim}{B}$, $\sum_{i=1}^{\nu-1} \sigma_i = 25$. From (9), $\sigma(\underset{\sim\sim}{B}\underset{\sim\sim}{R}\underset{\sim\sim}{B}^T) = \nu+2\sum_{i=1}^{\nu-1} \sigma_i$ $= 10 + 2 \times 25 = 60$. Similarly, $\sigma(\underset{\sim\sim}{M}\underset{\sim\sim}{R}\underset{\sim\sim}{M}^T) = 28$, $\sigma^*(\underset{\sim\sim}{Q}\underset{\sim\sim}{G}\underset{\sim\sim}{Q}^T) = 121$, $\sigma^*(\underset{\sim\sim}{A}\underset{\sim\sim}{G}\underset{\sim\sim}{A}^T) = 39$, and $\sigma^*(\hat{\underset{\sim\sim}{Q}}\underset{\sim\sim}{G}\hat{\underset{\sim\sim}{Q}}^T) = 31$.

This example also showed the following facts:

(a) the mesh (node) matrix usually results in sparser impedance (admittance) matrix than the fundamental loop (cut-set) matrix;

(b) the node admittance matrix does not always result in the sparsest coboundary admittance matrix.

IV. THE NEAREST NEIGHBOR ALGORITHM

We shall first define what is a local optimum cycle matrix with respect to the cycle basis graph; we do it by the following recursive definition:

Definition 8. A cycle matrix is a local optimum cycle matrix with respect to the cycle basis graph iff

(a) no neighbor of this cycle matrix has smaller σ value;

(b) all neighbors with same σ value must themselves satisfy (a) and (b).

From the above definition, it is obvious to formulate the algorithm as follows:

(a) given any cycle matrix, take it as the initial iteration matrix;

(b) check all the neighbors of the iteration matrix;

(c) if any neighbor has smaller σ value, take it as the new iteration matrix and go to (b); otherwise,

(d) if any neighbor has equal σ value and it has not been iterated on before, take it as the new iteration matrix and go to (b); otherwise,

(e) stop -- we have already reached a local optimum in the sense of Def. 8.

The flow chart for this algorithm is given in Fig. 3 and we shall use the example in Fig. 1(a) to illustrate this algorithm.

Let us start out with the fundamental loop matrix $\hat{B}_0$ with respect to the tree {6, 7, 8, 9, 10}. $\hat{B}_0$ is shown in Fig. 4(a) with the rightmost column containing the cycle matrix intersection coefficient σ_i's and the last row of this column containing $\sum_{i=1}^{\nu-1} \sigma_i$. From (9), $\sigma(\hat{B}_0 R \hat{B}_0^T) = 25$.

Iterate on $\hat{B}_0$, a neighbor with improvement in σ is shown in Fig. 4(b) (note, the σ value for this new cycle matrix is 19), take it as the new iteration matrix $\hat{B}_{01}$ and set Kiptrak = $\{\hat{B}_{01}\}$ where Kiptrak is the set containing all cycle matrices already iterated on that have the same σ as the current iteration matrix. Iterate on $\hat{B}_{01}$, a neighbor with improvement in σ is shown in Fig. 4(c) (σ = 17), take it as the new iteration matrix $\hat{B}_{02}$ and set Kiptrak = $\{\hat{B}_{02}\}$. Iterate on $\hat{B}_{02}$, another neighbor with improvement in σ is shown in Fig. 4(d) (σ = 15), take it as the new iteration matrix $\hat{B}_{03}$ and set Kiptrak = $\{\hat{B}_{03}\}$.

Iterate on $\hat{B}_{03}$, no neighbor with improvement in σ can be found; however, there

are several neighbors that have the same σ value as shown in Fig. 4(e), (f), (g), and (h). Take the matrix in Fig. 4(e) as the new iteration basis $\hat{\underset{\sim}{B}}_{04}$ while putting the matrices in Fig. 4(f), (g), and (h) into Minbase which is a set containing all cycle matrices not yet iterated on but have the same σ as the current iteration matrix. Set Kiptrak = $\{\hat{\underset{\sim}{B}}_{03}, \hat{\underset{\sim}{B}}_{04}\}$. Iterate on $\hat{\underset{\sim}{B}}_{04}$, again no neighbor with improvement can be found. Those neighbors, not in either Minbase or Kiptrak, but with same σ as $\hat{\underset{\sim}{B}}_{04}$ are shown in Fig. 4(i), (j), and (k). Take the matrix in Fig. 4(i) as the next iteration matrix $\hat{\underset{\sim}{B}}_{05}$ while adding the matrices in Fig. 4(j) and (k) to the set Minbase. Set Kiptrak = $\{\hat{\underset{\sim}{B}}_{03}, \hat{\underset{\sim}{B}}_{04}, \hat{\underset{\sim}{B}}_{05}\}$. Iterate on $\hat{\underset{\sim}{B}}_{05}$, again no improvement can be found. Those neighbors, not in Minbase or Kiptrak, but with same σ as $\hat{\underset{\sim}{B}}_{05}$ are shown in Fig. 4(ℓ), (m). Take the matrix in Fig. 4(ℓ) as the new iteration matrix $\hat{\underset{\sim}{B}}_{06}$ while putting the matrix in Fig. 4(m) into Minbase. Set Kiptrak = $\{\hat{\underset{\sim}{B}}_{03}, \hat{\underset{\sim}{B}}_{04}, \hat{\underset{\sim}{B}}_{05}, \hat{\underset{\sim}{B}}_{06}\}$. Iterate on $\hat{\underset{\sim}{B}}_{06}$, no improvement exists. Those neighbors, not in either Minbase or Kiptrak, but with same σ as $\hat{\underset{\sim}{B}}_{06}$ are shown in Fig. 4(n), (o). Take the matrix in Fig. 4(n) as the new iteration matrix $\hat{\underset{\sim}{B}}_{07}$ while adding the matrix in Fig. 4(o) to Minbase. Note, Minbase now contains the matrices in Figs. 4(f), (g), (h), (j), (k), (m), (o). Set Kiptrak = $\{\hat{\underset{\sim}{B}}_{03}, \hat{\underset{\sim}{B}}_{04}, \hat{\underset{\sim}{B}}_{05}, \hat{\underset{\sim}{B}}_{06}, \hat{\underset{\sim}{B}}_{07}\}$.

Iterate on $\hat{\underset{\sim}{B}}_{07}$, improvement can be found in the neighbor (σ = 13) as in Fig. 4(p). Take it as the next iteration matrix $\hat{\underset{\sim}{B}}_{08}$, and set Kiptrak = $\{\hat{\underset{\sim}{B}}_{08}\}$. Note, we also set Minbase = $\emptyset$ according to the algorithm. Iterate on $\hat{\underset{\sim}{B}}_{08}$, no improvement can be found, those neighbors, not in Kiptrak or Minbase, but have the same σ as $\hat{\underset{\sim}{B}}_{08}$ are shown in Fig. 4(q), (r). Take the neighbor in Fig. 4(q) as the next iteration matrix $\hat{\underset{\sim}{B}}_{09}$ while putting the neighbor in Fig. 4(r) into Minbase. Set Kiptrak = $\{\hat{\underset{\sim}{B}}_{08}, \hat{\underset{\sim}{B}}_{09}\}$. Iterate on $\hat{\underset{\sim}{B}}_{09}$, no improvement can be found, the neighbor, not in Kiptrak or Minbase, but have the same σ as $\hat{\underset{\sim}{B}}_{09}$ is shown in Fig. 4(s). Take it as the new iteration matrix $\hat{\underset{\sim}{B}}_{010}$ and set Kiptrak = $\{\hat{\underset{\sim}{B}}_{08}, \hat{\underset{\sim}{B}}_{09}, \hat{\underset{\sim}{B}}_{010}\}$. Iterate on $\hat{\underset{\sim}{B}}_{010}$, no improvement can be found; besides, no neighbor, not in Kiptrak or Minbase, but have the same σ as $\hat{\underset{\sim}{B}}_{010}$ can be found. Take the last element in Minbase, i.e., the cycle matrix in Fig. 4(r) (note, this is also the only element in Minbase at this time) as the next iteration matrix $\hat{\underset{\sim}{B}}_{011}$. Now Minbase contains one less element, hence becomes $\emptyset$. Set Kiptrak = $\{\hat{\underset{\sim}{B}}_{08}, \hat{\underset{\sim}{B}}_{09}, \hat{\underset{\sim}{B}}_{010}, \hat{\underset{\sim}{B}}_{011}\}$. Iterate on $\hat{\underset{\sim}{B}}_{011}$, no improvement can be found; besides, no neighbor, not in Kiptrak or Minbase, but have the same σ as $\hat{\underset{\sim}{B}}_{011}$ can be found. Since Minbase = $\emptyset$, this will terminate the algorithm with

$\hat{B}_{011}$ as the solution to this problem.

A flow diagram of the path of the above example is shown in Fig. 4(t). In the flow diagram, the arrow shows the direction of the path of iteration matrices, the alphabets correspond to the cycle matrices in Fig. 4, and the numbers correspond to the σ values of each cycle matrix. Note that only relevant neighbors are shown in the flow diagram. In the cycle basis graph for this example, every cycle matrix has $\nu(\nu-1)$ or 20 neighbors.

V. THE ROW-LENGTH MINIMIZATION ALGORITHM

The next algorithm is motivated by the idea that the less nonzero terms a row vector has, the less chances of this row vector being intersected by other row vectors. Hence, we associate this algorithm with the concept of row-length related basis graph.

Definition 9. The row-length related cycle basis graph is a subgraph of the cycle basis graph such that it has the same distinct cycle matrices in $\mathcal{Z}(G)$ as nodes and an oriented branch incident from node $\hat{B}$ to node $\hat{B}'$ iff

(a) $\hat{B}$ and $\hat{B}'$ are neighbors in the cycle basis graph $\mathcal{Z}(G)$;

(b) if $\hat{B}$ and $\hat{B}'$ differ by row k (note, $\hat{B}$ and $\hat{B}'$ differ by one and only one row in view of (a)), then length $(\hat{B}_k') \leq$ length $(\hat{B}_k)$ where length $(\hat{B}_k)$ is the number of nonzero terms in row k of $\hat{B}$.

Definition 10. From Def. 9, $\hat{B}'$ is said to be a successor of $\hat{B}$. $\hat{B}'$ is a proper successor of $\hat{B}$ if length $(\hat{B}_k') <$ length $(\hat{B}_k)$, and $\hat{B}'$ is a pseudo successor of $\hat{B}$ if length $(\hat{B}_k') =$ length $(\hat{B}_k)$.

Definition 11. A cycle matrix $\hat{B}$ is a local optimum with respect to the row-length related cycle basis graph iff

(a) no proper successor of $\hat{B}$ has equal or smaller σ;

(b) no pseudo successor of $\hat{B}$ has smaller σ.

From the above definitions, the row-length minimization algorithm is formulated as:

(a) given any cycle matrix, take it as the initial iteration matrix;

(b) find the row with maximal row length (i.e., maximal number of nonzero terms among the row vectors), take it as the iteration row;

(c) find all the successors with respect to the iteration row;

(d) if any proper successor has improving σ, take it as the new iteration matrix and go to (b); otherwise,

(e) if any proper successor has same σ, take it as the new iteration matrix and go to (b); otherwise,

(f) if any pseudo successor has improving σ, take it as the new iteration matrix and go to (b); otherwise,

(g) if there are rows that have not been iterated on, find the row with maximal length among them, take it as the new iteration row and go to (c); otherwise,

(h) stop -- we have already reached a local optimum in the sense of Def. 11.

The flow chart of this algorithm is given in Fig. 5 and we shall again use the example in Fig. 1(a) to illustrate this algorithm.

Let us start out with the same fundamental loop matrix $\hat{B}_0$ as in Fig. 4(a). The set containing the number of nonzero entries for each row of $\hat{B}_0$ is $RL(\hat{B}_0) = (3, 4, 4, 5, 6)$. Since $\ell_{max}=6$, $R_{max}=\{5\}$, $i_{max}=5$, we have $\underset{\sim}{\text{Mod2sum}}^1$ as in Fig. 6(a). The rightmost column of $\underset{\sim}{\text{Mod2sum}}^1$ is blank because we do not calculate σ for this matrix, and the fifth row is blank because we do not ring sum row 5 with itself. $RL'(\underset{\sim}{\text{Mod2sum}}^1) = (5, 4, 4, 3, -)$, $\ell_{min}=3$, $R'_{min}=\{4\}$, $k_{min}=4$, replace $(\hat{B}_0)_{i_{max}}$ by $(\underset{\sim}{\text{Mod2sum}}^1)_{k_{min}}$ and the result is in Fig. 6(b), denote it as $\hat{B}^1$. Note that $\hat{B}^1$ is a proper successor of $\hat{B}_0$ and has smaller σ value -- since from the last row of the rightmost column of Fig. 6(b) (which contains $\sum_{i=1}^{\nu-1} \sigma_i$) we have $\sigma(\hat{B}^1 R \hat{B}^{1T}) = 19$, while from Fig. 4(a) we have $\sigma(\hat{B}_0 R \hat{B}_0^T) = 25$. According to the algorithm, we take $\hat{B}^1$ as the next iteration matrix $\hat{B}_{01}$.

Iterate on $\hat{B}_{01}$, $RL(\hat{B}_{01}) = (3, 4, 4, 5, 3)$, $\ell_{max}=5$, $R_{max}=\{4\}$, $i_{max}=4$, and $\underset{\sim}{\text{Mod2sum}}^2$ is in Fig. 6(c). Since $RL'(\underset{\sim}{\text{Mod2sum}}^2) = (4, 3, 3, -, 6)$, $\ell_{min}=3$, $R'_{min}=\{2, 3\}$, $k_{min}=2$, we obtain $\hat{B}^2$ (as in Fig. 6(d)) by replacing $(\hat{B}_{01})_{i_{max}}$ by $(\underset{\sim}{\text{Mod2sum}}^2)_{k_{min}}$. $\hat{B}^2$ is a proper successor of $\hat{B}_{01}$, and since it has improving σ value ($\sigma=15$), we take it as the next iteration matrix $\hat{B}_{02}$.

Iterate on $\hat{B}_{02}$, $RL(\hat{B}_{02}) = (3, 4, 4, 3, 3)$, $\ell_{max}=4$, $R_{max}=\{2,3\}$, $i_{max}=2$, and $\underset{\sim}{\text{Mod2sum}}^3$ is in Fig. 6(e). Since $RL'(\underset{\sim}{\text{Mod2sum}}^3) = (3, -, 2, 5, 7)$, $\ell_{min}=2$ $R'_{min}=\{3\}$, $k_{min}=3$, we obtain $\hat{B}^3$ (as in Fig. 6(f)) by replacing $(\hat{B}_{02})_{i_{max}}$ by $(\underset{\sim}{\text{Mod2sum}}^3)_{k_{min}}$. $\hat{B}^3$ is a proper successor of $\hat{B}_{02}$, and since it has improving σ value ($\sigma=13$), we take it as the next iteration matrix $\hat{B}_{03}$.

Iterate on $\hat{B}_{03}$, $RL(\hat{B}_{03}) = (3, 2, 4, 3, 3)$, $\ell_{max}=4$, $R_{max}=\{3\}$, $i_{max}=3$, and $\underset{\sim}{\text{Mod2sum}}^4$ is in Fig. 6(g). Since $RL'(\underset{\sim}{\text{Mod2sum}}^4) = (3, 4, -, 7, 7)$, $\ell_{min}=3$,

$R'_{min}=\{1\}$, $k_{min}=1$, we obtain $\hat{\underset{\sim}{B}}^4$ (as in Fig. 6(h)) by replacing $(\hat{\underset{\sim}{B}}_{03})_{i_{max}}$ by $(\underset{\sim}{\text{Mod2sum}}^4)_{k_{min}}$. $\hat{\underset{\sim}{B}}^4$ is a proper successor of $\hat{\underset{\sim}{B}}_{03}$, and since it has same $\sigma(\sigma=13)$, we take it as the next iteration matrix $\hat{\underset{\sim}{B}}_{04}$.

Iterate on $\hat{\underset{\sim}{B}}_{04}$, $RL(\hat{\underset{\sim}{B}}_{04}) = (3, 2, 3, 3, 3)$, $\ell_{max}=3$, $R_{max}=\{1, 3, 4, 5\}$, $i_{max}=1$, and $\underset{\sim}{\text{Mod2sum}}^5$ is in Fig. 6(i). Since $RL'(\underset{\sim}{\text{Mod2sum}}^5) = (-, 5, 4, 6, 6)$, $\ell_{min}=4 > \ell_{max}$, we take the next element in R_{max} as i_{max}, i.e., $i_{max}=3$. Then $\underset{\sim}{\text{Mod2sum}}^6$ is in Fig. 6(j). Since $RL'(\underset{\sim}{\text{Mod2sum}}^6) = (4, 3, -, 6, 6)$, $\ell_{min}=3=\ell_{max}$, $R'_{min}=\{2\}$, $k_{min}=2$, we obtain $\hat{\underset{\sim}{B}}^5$ (as in Fig. 6(k)) by replacing $(\hat{\underset{\sim}{B}}_{04})_{i_{max}}$ by $(\underset{\sim}{\text{Mod2sum}}^6)_{k_{min}}$. $\hat{\underset{\sim}{B}}^5$ is a pseudo successor of $\hat{\underset{\sim}{B}}_{04}$, and since it has larger σ value $(\sigma=15)$, take the next element in R_{max} as i_{max}, i.e., $i_{max}=4$. Then $\underset{\sim}{\text{Mod2sum}}^7$ is in Fig. 6(ℓ). Since $RL'(\underset{\sim}{\text{Mod2sum}}^7) = (6, 3, 6, -, 4)$, $\ell_{min}=3=\ell_{max}$, $R'_{min}=\{2\}$, $k_{min}=2$, we obtain $\hat{\underset{\sim}{B}}^6$ (as in Fig. 6(m)) by replacing $(\hat{\underset{\sim}{B}}_{04})_{i_{max}}$ by $(\underset{\sim}{\text{Mod2sum}}^7)_{k_{min}}$. $\hat{\underset{\sim}{B}}^6$ is a pseudo successor of $\hat{\underset{\sim}{B}}_{04}$, and since it has larger σ value $(\sigma=15)$, take the next element in R_{max} as i_{max}, i.e., $i_{max}=5$. Then $\underset{\sim}{\text{Mod2sum}}^8$ is in Fig. 6(n). Since $RL'(\underset{\sim}{\text{Mod2sum}}^8) = (6, 5, 6, 4, -)$, $\ell_{min}=4>\ell_{max}$, and because no more element left in R_{max}, we re-evaluate RL as $RL(\hat{\underset{\sim}{B}}_{04}) = (-, 2, -, -, -)$, $\ell_{max}=2$, $R_{max}=\{2\}$, $i_{max}=2$, and $\underset{\sim}{\text{Mod2sum}}^9$ is in Fig. 6(o). Since $RL'(\underset{\sim}{\text{Mod2sum}}^9) = (5, -, 3, 3, 5)$, $\ell_{min}=3>\ell_{max}$, we re-evaluate RL as $RL(\hat{\underset{\sim}{B}}_{04}) = (-, -, -, -, -)$. Since $RL(\hat{\underset{\sim}{B}}_{04}) = \emptyset$, this terminates the algorithm.

A flow diagram of the path of this algorithm is included in Fig. 6(p). In the flow diagram, single-arrowed branch leads to proper successors, and double-arrowed branch leads to pseudo successors. The ordered 5-tuple near each node is the row length associated with it.

VI. A SUBOPTIMAL NONPLANAR ALGORITHM

This is a generalized version of mesh analysis in nonplanar networks. The basic concept is to find the maximal planar subgraph, take the meshes of this subgraph as part of the cycle basis. The remainder of the cycle basis is filled when the original nonplanar graph is constructed from its maximal planar subgraph. The algorithm formulates as follows:

(a) number the branches of the graph $\mathcal{G}$ arbitrarily from 1 to b (assume b branches in $\mathcal{G}$);

(b) let subgraph $\mathcal{G}_0$ contain only nodes of $\mathcal{G}$ and no branches, let i=1;

(c) add branch i to subgraph $\mathcal{G}_{i-1}$; if branch i makes the resulting graph nonplanar, store i in the set Nonplanar and $\mathcal{G}_i = \mathcal{G}_{i-1}$, otherwise

$\mathcal{G}_i = \mathcal{G}_{i-1} \cup$ branch i;

(d) i = i+1, if i $\leq$ b, go to (c), otherwise,

(e) let $\underset{\sim}{M}_0$ be the mesh matrix of subgraph $\mathcal{G}_b$, let CL($\underset{\sim}{M}_0$) be the set containing the number of nonzero terms in each column of $\underset{\sim}{M}_0$, let j=1;

(f) we obtain subgraph $\mathcal{G}_{b+j}$ by adding branch (Nonplanar (j)) to subgraph $\mathcal{G}_{b+j-1}$: find a cycle $\mathcal{Z}_j$ containing branch (Nonplanar (j)) such that the row length of $\mathcal{Z}_j$ is minimal and in the resulting graph $\mathcal{Z}_j$ will leave the number of entries of CL($\underset{\sim}{M}_j$) as small as possible where $\underset{\sim}{M}_j = \underset{\sim}{M}_{j-1} \cup \mathcal{Z}_j$;

(g) j = j+1, if j $\leq$ |Nonplanar| (i.e., cardinality of the set Nonplanar); go to (f), otherwise,

(h) stop, $\mathcal{G}_{b+|\text{Nonplanar}|} = \mathcal{G}$ and we have reached a suboptimal basis.

We shall illustrate this algorithm by the example shown in Fig. 7(a). The maximal planar subgraph $\mathcal{G}_{15}$ is shown in Fig. 7(b), the associated mesh matrix $\underset{\sim}{M}_0$ is shown in first seven rows of Fig. 7(f), and the column length of $\underset{\sim}{M}_0$ is shown in the eleventh row of Fig. 7(f) denoted by CL($\underset{\sim}{M}_0$). The set Nonplanar contains three elements {13, 14, 15}.

For j=1, Nonplanar (1) = 13, $\mathcal{G}_{16}$ is shown in Fig. 7(c). Observe $\mathcal{G}_{16}$ carefully and we will find only one cycle containing branch 13 that has row length = 3; namely, $\mathcal{Z}_1$ = {6, 9, 13}. We obtain $\underset{\sim}{M}_1$ by adding $\mathcal{Z}_1$ to $\underset{\sim}{M}_0$, i.e., putting $\mathcal{Z}_1$ in the eighth row of Fig. 7(f). The column length of $\underset{\sim}{M}_1$ is shown in the twelfth row of Fig. 7(f) denoted by CL($\underset{\sim}{M}_1$).

For j=2, Nonplanar (2) = 14, $\mathcal{G}_{17}$ is shown in Fig. 7(d). Observe $\mathcal{G}_{17}$ carefully and we will find there are four cycles containing branch 14 that have row length = 3; namely, $\mathcal{Z}_2^1$ = {5, 13, 14}, $\mathcal{Z}_2^2$ = {3, 4, 14}, $\mathcal{Z}_2^3$ = {7, 9, 14}, and $\mathcal{Z}_2^4$ = {2, 11, 14}. Among them, both $\mathcal{Z}_2^1$ and $\mathcal{Z}_2^2$ will yield CL($\underset{\sim}{M}_2$) with entries as small as possible. The choice here is arbitrary, we put $\mathcal{Z}_2^1$ in the ninth row of Fig. 7(f) and CL($\underset{\sim}{M}_2$) with respect to $\mathcal{Z}_2^1$ is shown in the thirteenth row of Fig. 7(f).

For j=3, Nonplanar (3)=15, $\mathcal{G}_{18}$ is shown in Fig. 7(e). Observe $\mathcal{G}_{18}$ carefully and we will find there are four cycles containing branch 15 that has row length = 3; namely, $\mathcal{Z}_3^1$ = {4, 5, 15}, $\mathcal{Z}_3^2$ = {6, 8, 15}, $\mathcal{Z}_3^3$ = {3, 13, 15}, and $\mathcal{Z}_3^4$ = {10, 12, 15}. Among them, $\mathcal{Z}_3^4$ will yield CL($\underset{\sim}{M}_3$) with entries as small as possible. $\mathcal{Z}_3^4$ is put in the tenth row of Fig. 7(f) and the corresponding CL($\underset{\sim}{M}_3$) is shown in the fourteenth row of Fig. 7(f). The <u>generalized mesh matrix</u> $\underset{\sim}{\hat{M}}$ is same as $\underset{\sim}{M}_3$ and is shown in the first ten rows of Fig. 7(f).

In the rightmost column of Fig. 7(f), we have the values of σ_i's, and $\sum_{i=1}^{\nu-1} \sigma_i$ is denoted by "$\sum$" = 19, therefore $\sigma(\hat{\underset{\sim}{M}}\underset{\sim}{R}\hat{\underset{\sim}{M}}^T) = 48$. Take a fundamental loop matrix $\underset{\sim}{B}$ with respect to the tree {1, 2, 3, 4, 5} as shown in Fig. 7(g), we have $\sigma(\underset{\sim}{B}\underset{\sim}{R}\underset{\sim}{B}^T) = 90$. $\hat{\underset{\sim}{M}}$ results in obviously sparser cycle impedance matrix than $\underset{\sim}{B}$.

VII. CONCLUSION

Another algorithm based on the idea that a column with k nonzero elements will contribute $2\sum_{i=1}^{k-1} i$ to the σ value has been explored. This approach is called the column-length minimization algorithm. So far, this approach yields results not very fruitful.

Comparing the nearest neighbor algorithm (Alg. 1) with the row-length minimization algorithm (Alg. 2), we find Alg. 2 is more efficient than Alg. 1 because Alg. 2 does not need to calculate σ values for all $\nu(\nu-1)$ neighbors while Alg. 1 does. However, the local optimum of Alg. 2 is usually not as sparse as the local optimum of Alg. 1. A hybrid model of algorithms can utilize the advantages of both Algs. 1 and 2; i.e., to start with Alg. 2 while finishing up with Alg. 1. Nevertheless, this hybrid model will not work out for matrices of dimension $\nu > 15$ very efficiently.

Because of the problem that local optimum with respect to the basis graph is not the global optimum (see Appendix B), an efficient global optimum algorithm (see Appendix C) is not found yet. However, in most practical studies, the local optimum seems to be very close to the global optimum such that it is not worthwhile to implement a global algorithm even if one exists. Nevertheless, from the theoretical standpoint, such a global algorithm would be desirable.

Appendix A. Computing μ_i

Assume there is only one nondiagonal term in $\underset{\sim}{R}$, let it be $R_{pq} \neq 0$, $p \neq q$.

Definition A-1. $\mu_{ij} = 1$ iff

(a) $\hat{\underset{\sim}{B}}_i \cap \hat{\underset{\sim}{B}}_j = \emptyset$

(b) $(\hat{\underset{\sim}{B}}_i \underset{\sim}{R}) \cap \hat{\underset{\sim}{B}}_j \neq \emptyset$

From Def. A-1, it is obvious that $\mu_i = \sum_{j \neq i} \mu_{ij}$.

Theorem A-1. $\mu_{ij} = 1$ iff $\hat{B}_{iq} \neq 0$ and $\hat{B}_{jp} \neq 0$

Proof: If $\hat{B}_{iq} = 0$, then $\mu_{ij} = 0$. If $\hat{B}_{iq} \neq 0$, $\hat{B}_{jp} = 0$ then $\mu_{ij} = 0$. If $\hat{B}_{iq} \neq 0$, $\hat{B}_{jp} \neq 0$, $\hat{B}_{jq} \neq 0$, then this is contradictory since $\hat{B}_i \cap \hat{B}_j = \emptyset$. If $\hat{B}_{iq} \neq 0$, $\hat{B}_{jp} \neq 0$, $\hat{B}_{jq} = 0$, then $\mu_{ij} = 1$. Therefore $B_{iq} \neq 0$, $B_{jp} \neq 0$ iff $\mu_{ij} = 1$.

□

Appendix B. Local Optimum is not Global Optimum

Consider the example in Fig. A-1(a), let $\underset{\sim}{M}$ be the mesh matrix as in Fig. A-1(b), we find $\sigma(\underset{\sim}{M}\underset{\sim}{R}\underset{\sim}{M}^T) = 89$. Let $\hat{\underset{\sim}{B}}$ be the cycle matrix shown in Fig. A-1(c), we can obtain $\hat{\underset{\sim}{B}}$ from $\underset{\sim}{M}$ by adding the eighth row through the seventeenth row except the sixteenth row and replacing the seventeenth row by the ring sum. $\sigma(\hat{\underset{\sim}{B}}\underset{\sim}{R}\hat{\underset{\sim}{B}}^T) = 87$. Through exhaustive checking of $\underset{\sim}{M}$'s neighbors, we will find $\underset{\sim}{M}$ is a local optimum with respect to the cycle basis graph. However, $\underset{\sim}{M}$ is not the global optimum because of the existence of $\hat{\underset{\sim}{B}}$.

Appendix C. Enumerating all Distinct Cycle Basis

The flow chart to enumerate all $N_\nu \triangleq \frac{1}{\nu!} \prod_{i=0}^{\nu-1} (2^\nu - 2^i)$ distinct cycle matrices without redundancy is presented in Fig. A-2(a). And the flow chart to determine the global optimum cycle matrix $\hat{B}_{opt}$ is presented in Fig. A-2(b).

REFERENCES

1. C. A. Desoer and E. S. Kuh, Basic Circuit Theory. New York: McGraw-Hill, 1969.
2. D. A. Calahan, Computer-Aided Network Design. Revised Edition. New York: McGraw-Hill, 1972.
3. A. N. Willson, Jr., "On the Solutions of Equations for Nonlinear Resistive Networks," Bell Syst. Tech. J., Vol. 47, Oct. 1968, pp. 1755 - 1773.
4. I. W. Sandberg and A. N. Willson, Jr., "Some Theorems on Properties of DC Equations of Nonlinear Networks," Bell Syst. Tech. J., Vol 48, pp. 1 - 34, January 1969.
5. T. Fujisawa and E. S. Kuh, "Some Results on Existence and Uniqueness of Solutions of Nonlinear Networks," IEEE Trans. Circuit Theory, Vol. CT-18, No. 5, pp. 501 - 506, September 1971.
6. S. Seshu and M. B. Reed, Linear Graphs and Electrical Network. Mass.: Addison-Wesley, 1961.
7. C. Berge and A. Ghouila-Houri, Programming, Games and Transportation Networks. New York: Wiley, 1962.
8. F. Harary, Graph Theory. Mass.: Addison-Wesley, 1969.
9. W. K. Chen, Applied Graph Theory. Amsterdam: North-Holland, 1971.
10. W. Mayeda, Graph Theory. New York: Wiley, 1972.

FOOTNOTES

1. To conserve space, all symbols and notations in this paper that are not defined are used as in [1].
2. We consider a linear resistive network here for convenience. Equation (3) applies, of course, also to a linear RLC network with $\underset{\sim}{R}$ replaced by the branch impedance matrix $\underset{\sim}{Z}$.
3. The term "cycle" ("coboundary") may not be too familiar in circuit theory literature; but they appear to be more descriptive since a cycle (coboundary) is generally the union of disjoint loops (cut-sets). The terminologies adopted in this section are well known in graph-theoretic literatures [7 - 8].

LIST OF FIGURE CAPTIONS

Fig. 1 (a) A network with current-controlled resistors. (b) Fundamental loop matrix w.r.t. tree {6, 7, 8, 9, 10}. (c) Mesh matrix w.r.t. meshes {①, ②, ③, ④, ⑤}.

Fig. 2 (a) An illustrative example. (b) Fundamental loop matrix $\underset{\sim}{B}$ w.r.t. tree {11, 12, . . ., 21}. (c) Mesh matrix $\underset{\sim}{M}$. (d) Fundamental cut-set matrix $\underset{\sim}{Q}$ w.r.t. tree {11, 12, . . ., 21}. (e) Reduced incidence matrix $\underset{\sim}{A}$. (f) Coboundary matrix $\hat{\underset{\sim}{Q}}$.

Fig. 3 Flow chart of the nearest neighbor algorithm.

Fig. 4 (a) $\hat{\underset{\sim}{B}}_0$ (b) $\hat{\underset{\sim}{B}}_{01}$ (c) $\hat{\underset{\sim}{B}}_{02}$ (d) $\hat{\underset{\sim}{B}}_{03}$ (e) $\hat{\underset{\sim}{B}}_{04}$ (f) $\underset{\sim}{\text{Minbase}}_1$ (g) $\underset{\sim}{\text{Minbase}}_2$ (h) $\underset{\sim}{\text{Minbase}}_3$ (i) $\hat{\underset{\sim}{B}}_{05}$ (j) $\underset{\sim}{\text{Minbase}}_4$ (k) $\underset{\sim}{\text{Minbase}}_5$ (ℓ) $\hat{\underset{\sim}{B}}_{06}$ (m) $\underset{\sim}{\text{Minbase}}_6$ (n) $\hat{\underset{\sim}{B}}_{07}$ (o) $\underset{\sim}{\text{Minbase}}_7$ (p) $\hat{\underset{\sim}{B}}_{08}$ (q) $\hat{\underset{\sim}{B}}_{09}$ (r) $\underset{\sim}{\text{Minbase}}_1$ and $\hat{\underset{\sim}{B}}_{011}$ (s) $\hat{\underset{\sim}{B}}_{010}$ (t) flow diagram.

Fig. 5 Flow chart of the row-length minimization algorithm.

Fig. 6 (a) $\underset{\sim}{\text{Mod2sum}}^1$ (b) $\hat{\underset{\sim}{B}}^1$ and $\hat{\underset{\sim}{B}}_{01}$ (c) $\underset{\sim}{\text{Mod2sum}}^2$ (d) $\hat{\underset{\sim}{B}}^2$ and $\hat{\underset{\sim}{B}}_{02}$ (e) $\underset{\sim}{\text{Mod2sum}}^3$ (f) $\hat{\underset{\sim}{B}}^3$ and $\hat{\underset{\sim}{B}}_{03}$ (g) $\underset{\sim}{\text{Mod2sum}}^4$ (h) $\hat{\underset{\sim}{B}}^4$ and $\hat{\underset{\sim}{B}}_{04}$ (i) $\underset{\sim}{\text{Mod2sum}}^5$ (j) $\underset{\sim}{\text{Mod2sum}}^6$ (k) $\hat{\underset{\sim}{B}}^5$ (ℓ) $\underset{\sim}{\text{Mod2sum}}^7$ (m) $\hat{\underset{\sim}{B}}^6$ (n) $\underset{\sim}{\text{Mod2sum}}^8$ (o) $\underset{\sim}{\text{Mod2sum}}^9$ (p) flow diagram

Fig. 7 (a) $\mathcal{G}$ (b) $\mathcal{G}_{15}$ (c) $\mathcal{G}_{16}$ (d) $\mathcal{G}_{17}$ (e) $\mathcal{G}_{18}$ (f) Generalized mesh matrix $\hat{\underset{\sim}{M}}$. (g) Fundamental loop matrix w.r.t. tree {1, 2, 3, 4, 5}.

Fig. A-1 An illustrative example. (b) Mesh matrix $\underset{\sim}{M}$. (c) Cycle matrix $\hat{\underset{\sim}{B}}$.

Fig. A-2 (a) Flow chart for enumerating all basis. (b) Flow chart for generating σ_{opt}.

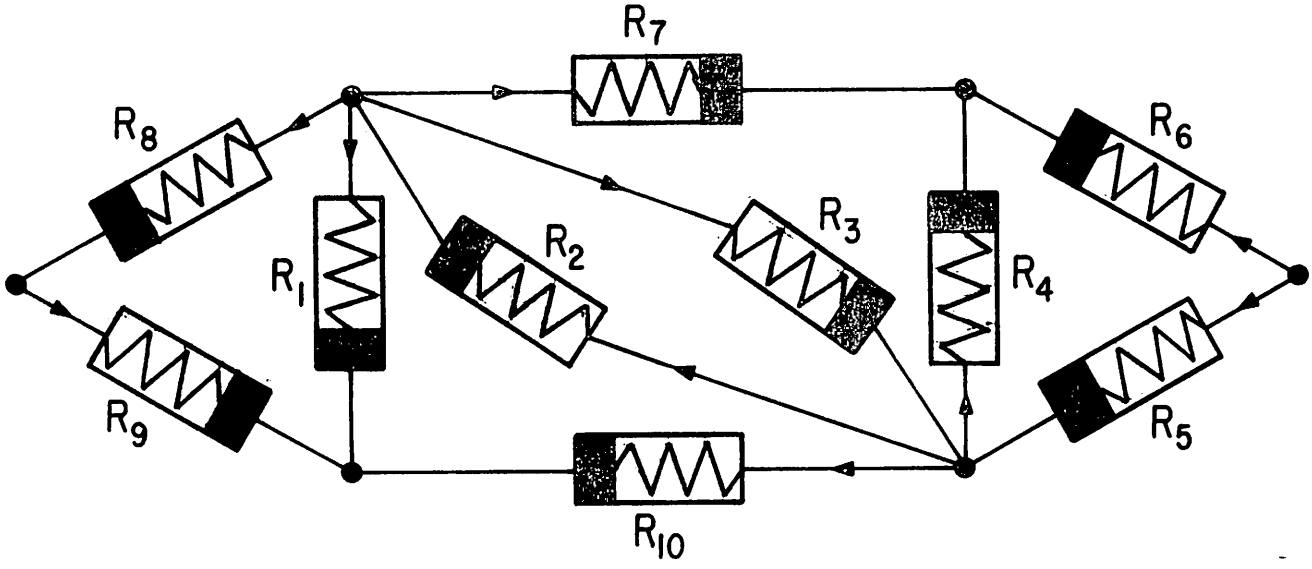

(a)

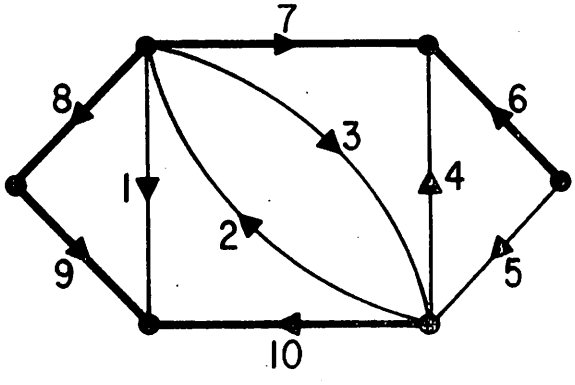

+1							-1	-1	
	+1						+1	+1	-1
		+1					-1	-1	+1
			+1			-1	+1	+1	-1
				+1	-1	+1	-1	-1	+1

(b)

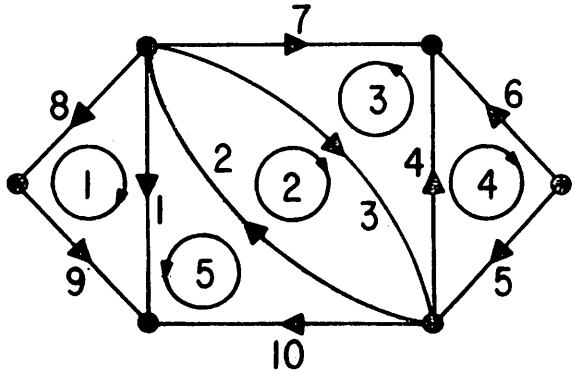

+1							-1	-1	
	+1	+1							
		+1	+1			-1			
			+1	+1	-1				
+1	+1								-1

(c)

Fig. 1

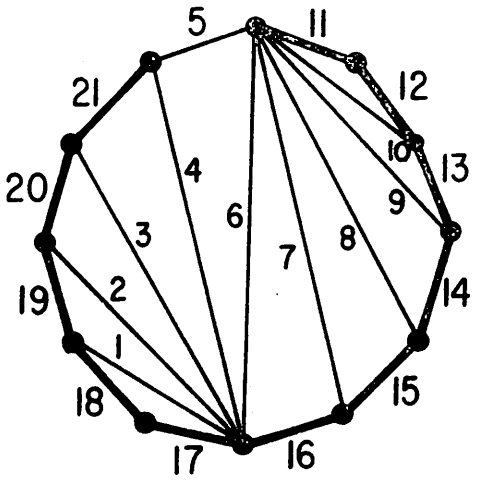

(a)

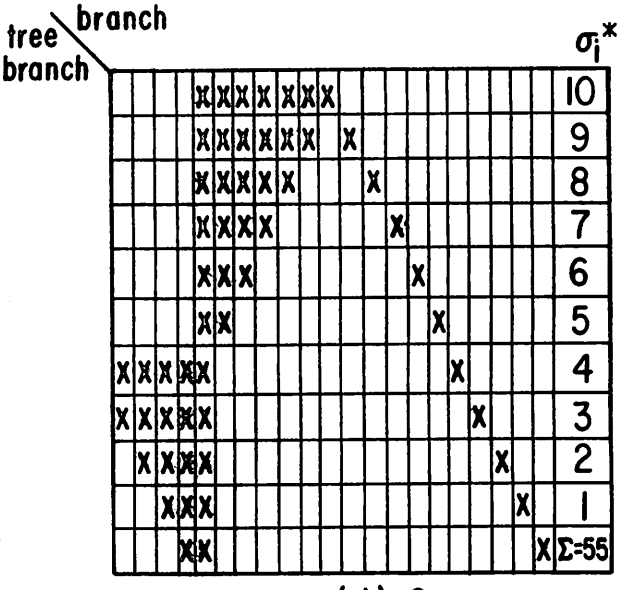

(d) $\underset{\sim}{Q}$

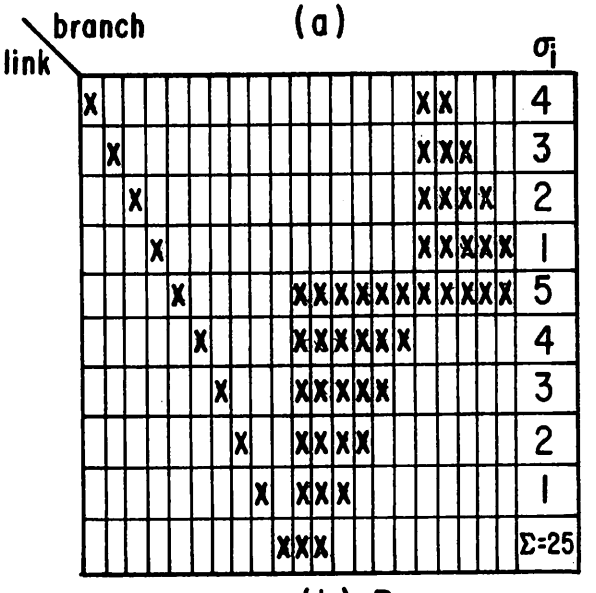

(b) $\underset{\sim}{B}$

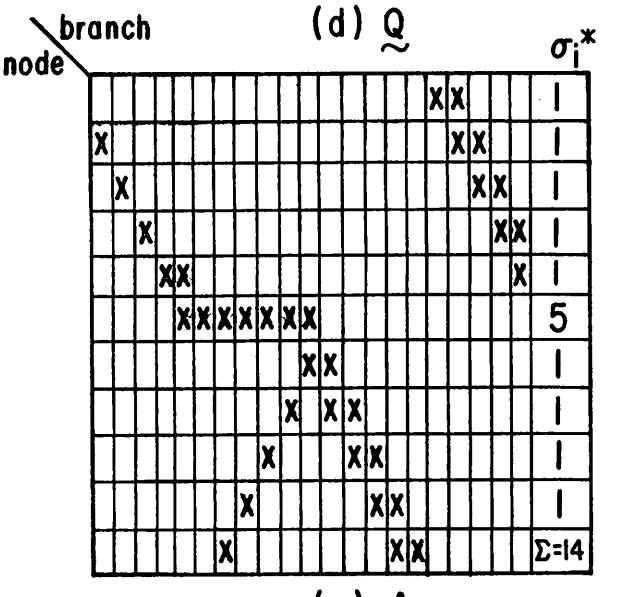

(e) $\underset{\sim}{A}$

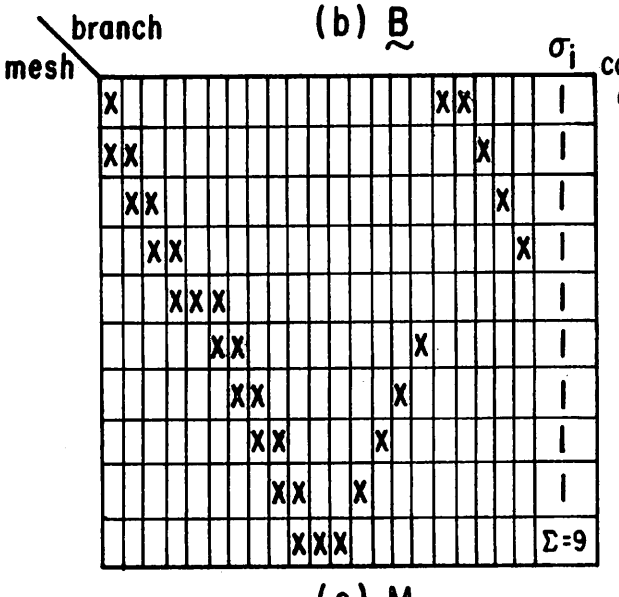

(c) $\underset{\sim}{M}$

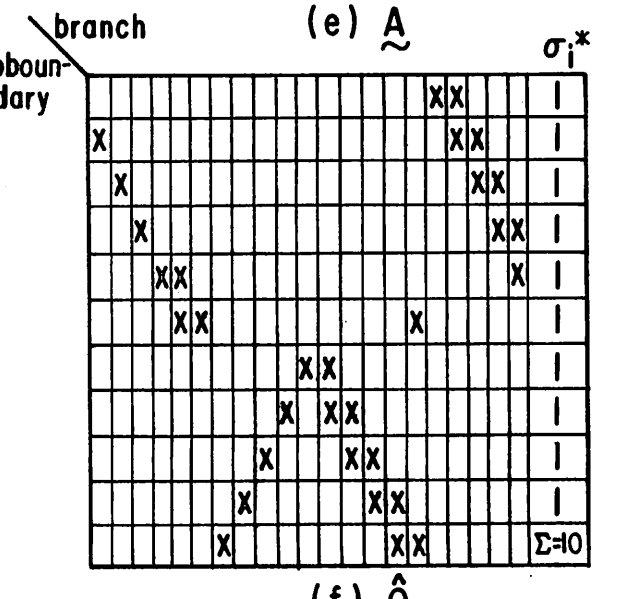

(f) $\hat{\underset{\sim}{Q}}$

Fig. 2

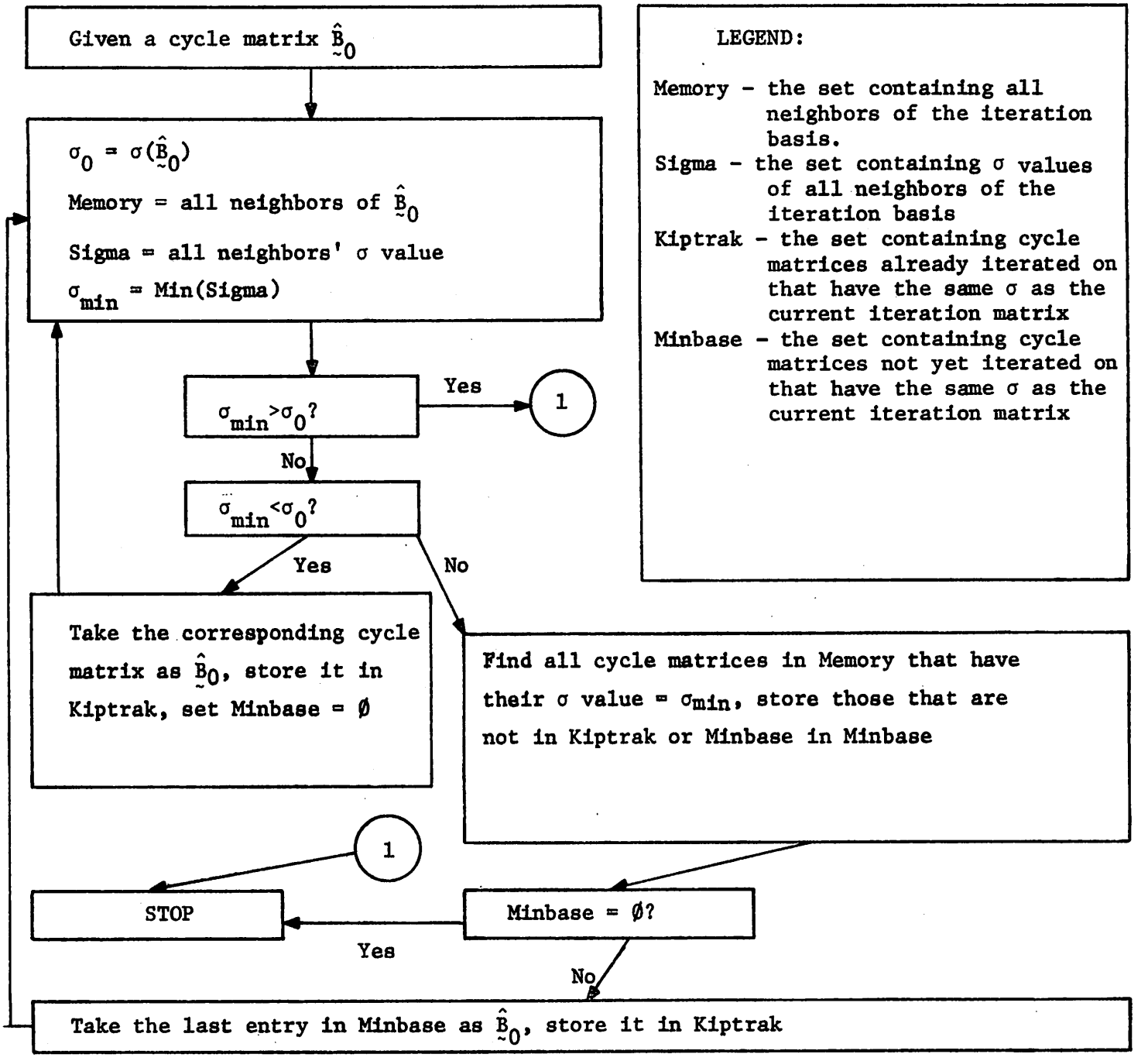
Given a cycle matrix $\hat{B}_0$
$\sigma_0 = \sigma(\hat{B}_0)$
Memory = all neighbors of $\hat{B}_0$
Sigma = all neighbors' σ value
σ_{min} = Min(Sigma)
$\sigma_{min} > \sigma_0$?
Yes
1
No
$\sigma_{min} < \sigma_0$?
Yes
No
Take the corresponding cycle matrix as $\hat{B}_0$, store it in Kiptrak, set Minbase = ∅
Find all cycle matrices in Memory that have their σ value = σ_{min}, store those that are not in Kiptrak or Minbase in Minbase
1
STOP
Minbase = ∅?
Yes
No
Take the last entry in Minbase as $\hat{B}_0$, store it in Kiptrak
LEGEND:
Memory - the set containing all neighbors of the iteration basis.
Sigma - the set containing σ values of all neighbors of the iteration basis
Kiptrak - the set containing cycle matrices already iterated on that have the same σ as the current iteration matrix
Minbase - the set containing cycle matrices not yet iterated on that have the same σ as the current iteration matrix

Fig. 3

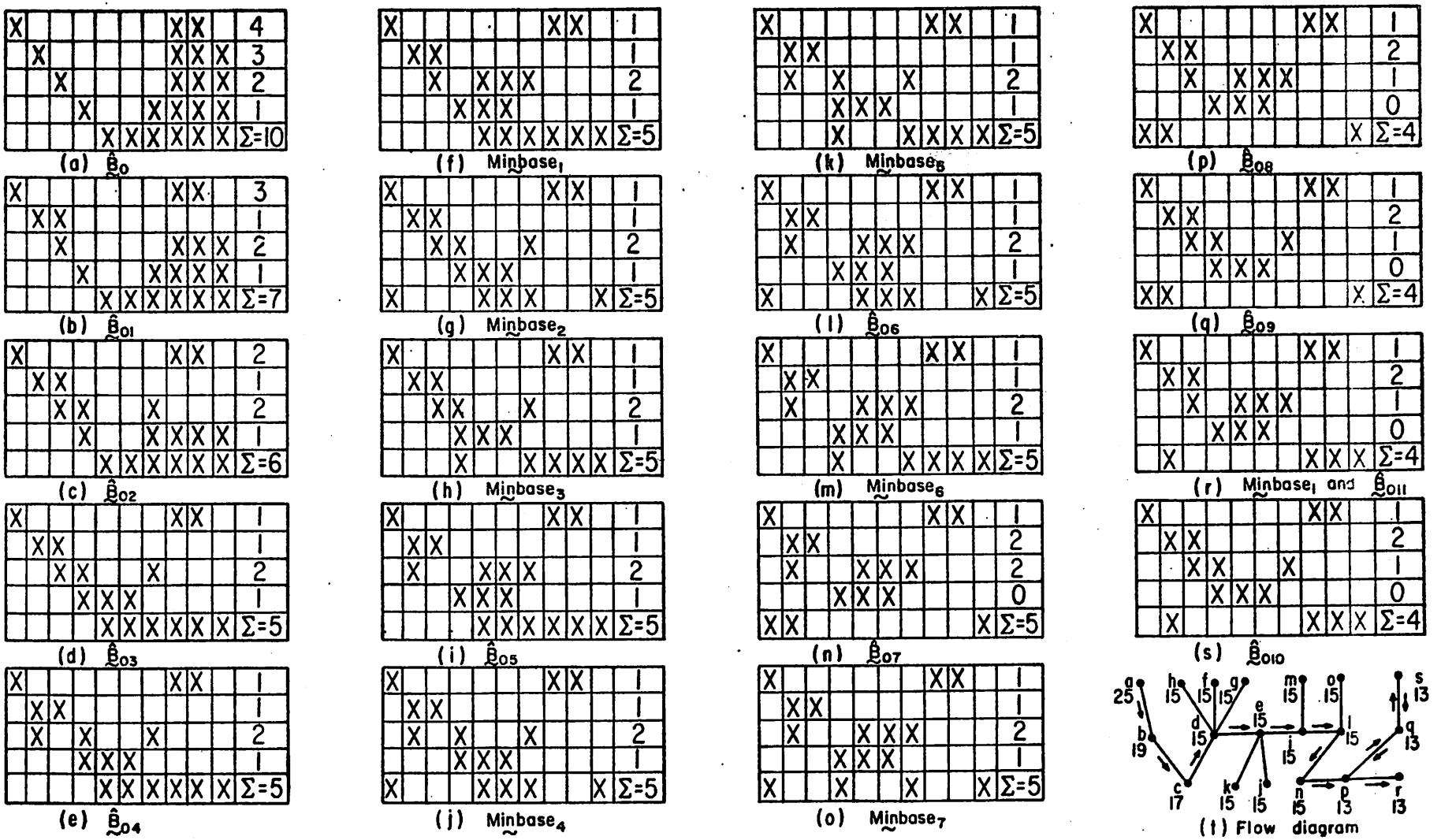
(a) $\hat{B}_0$
(b) $\hat{B}_{01}$
(c) $\hat{B}_{02}$
(d) $\hat{B}_{03}$
(e) $\hat{B}_{04}$
(f) Minbase$_1$
(g) Minbase$_2$
(h) Minbase$_3$
(i) $\hat{B}_{05}$
(j) Minbase$_4$
(k) Minbase$_5$
(l) $\hat{B}_{06}$
(m) Minbase$_6$
(n) $\hat{B}_{07}$
(o) Minbase$_7$
(p) $\hat{B}_{08}$
(q) $\hat{B}_{09}$
(r) Minbase$_1$ and $\hat{B}_{011}$
(s) $\hat{B}_{010}$
(t) Flow diagram

Fig. 4

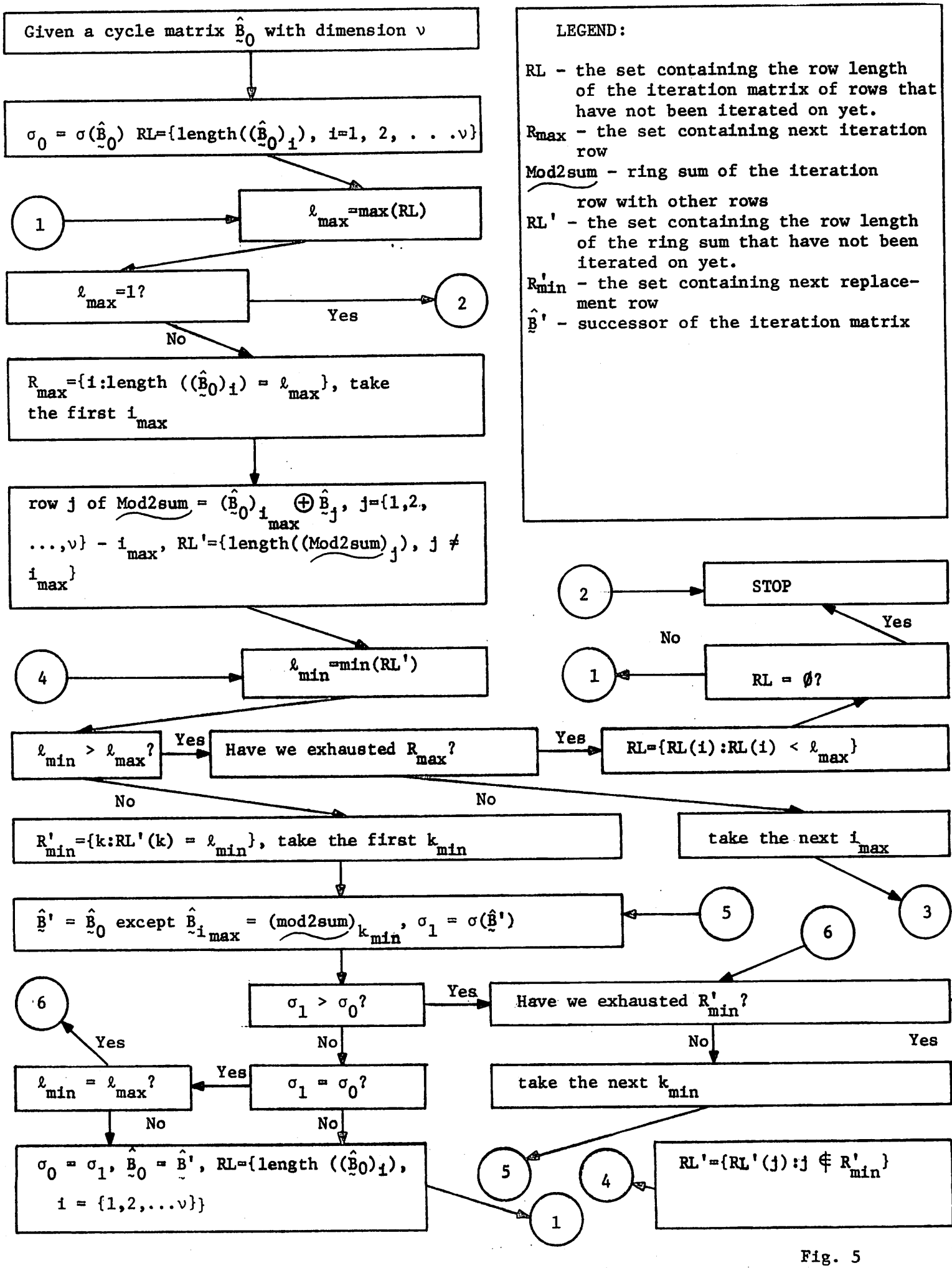
Given a cycle matrix $\hat{B}_0$ with dimension ν
$\sigma_0 = \sigma(\hat{B}_0)$ RL={length$((\hat{B}_0)_i)$, i=1, 2, . . .ν}
1
ℓ_{max}=max(RL)
ℓ_{max}=1?
Yes
2
No
R_{max}={i:length $((\hat{B}_0)_i) = \ell_{max}$}, take the first i_{max}
row j of Mod2sum = $(\hat{B}_0)_{i_{max}} \oplus \hat{B}_j$, j={1,2, ...,ν} - i_{max}, RL'={length$((Mod2sum)_j)$, j ≠ i_{max}}
4
ℓ_{min}=min(RL')
$\ell_{min} > \ell_{max}$?
Yes
Have we exhausted R_{max}?
Yes
RL={RL(i):RL(i) < ℓ_{max}}
No
No
R'_{min}={k:RL'(k) = ℓ_{min}}, take the first k_{min}
take the next i_{max}
$\hat{B}' = \hat{B}_0$ except $\hat{B}_{i_{max}} = (mod2sum)_{k_{min}}$, $\sigma_1 = \sigma(\hat{B}')$
5
6
3
6
$\sigma_1 > \sigma_0$?
Yes
Have we exhausted R'_{min}?
Yes
No
No
Yes
$\ell_{min} = \ell_{max}$?
Yes
$\sigma_1 = \sigma_0$?
No
No
take the next k_{min}
$\sigma_0 = \sigma_1$, $\hat{B}_0 = \hat{B}'$, RL={length $((\hat{B}_0)_i)$, i = {1,2,...ν}}
5
4
$RL'=\{RL'(j):j \notin R'_{min}\}$
1
2
STOP
Yes
No
1
RL = ∅?
LEGEND:
RL - the set containing the row length of the iteration matrix of rows that have not been iterated on yet.
R_{max} - the set containing next iteration row
Mod2sum - ring sum of the iteration row with other rows
RL' - the set containing the row length of the ring sum that have not been iterated on yet.
R'_{min} - the set containing next replacement row
$\hat{B}'$ - successor of the iteration matrix

Fig. 5

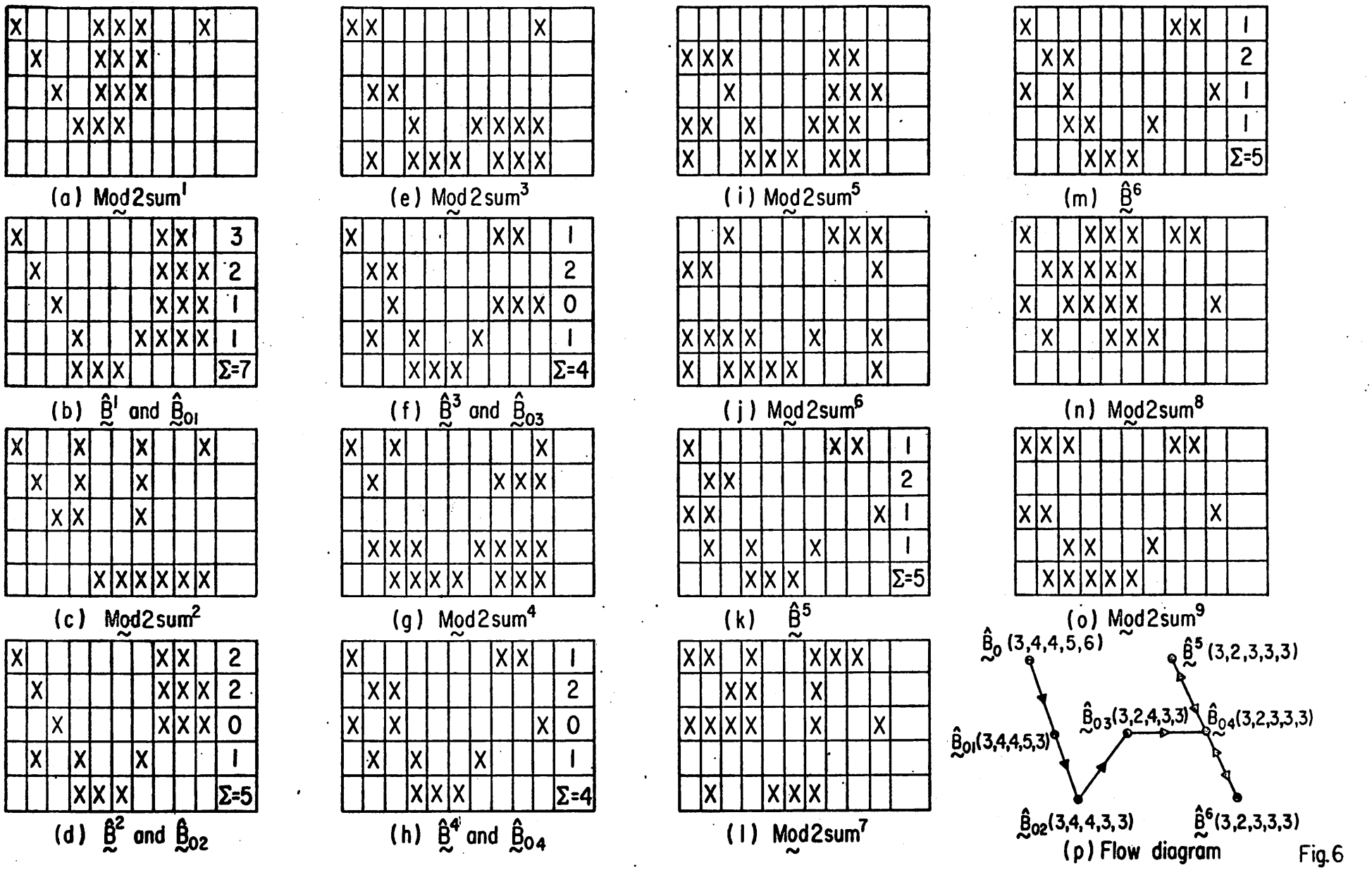
(a) Mod2sum¹
(b) $\hat{B}^1$ and $\hat{B}_{01}$
(c) Mod2sum²
(d) $\hat{B}^2$ and $\hat{B}_{02}$
(e) Mod2sum³
(f) $\hat{B}^3$ and $\hat{B}_{03}$
(g) Mod2sum⁴
(h) $\hat{B}^4$ and $\hat{B}_{04}$
(i) Mod2sum⁵
(j) Mod2sum⁶
(k) $\hat{B}^5$
(l) Mod2sum⁷
(m) $\hat{B}^6$
(n) Mod2sum⁸
(o) Mod2sum⁹
$\hat{B}_0$ (3,4,4,5,6)
$\hat{B}^5$ (3,2,3,3,3)
$\hat{B}_{03}$(3,2,4,3,3)
$\hat{B}_{04}$(3,2,3,3,3)
$\hat{B}_{01}$(3,4,4,5,3)
$\hat{B}_{02}$(3,4,4,3,3)
$\hat{B}^6$(3,2,3,3,3)
(p) Flow diagram

Fig.6

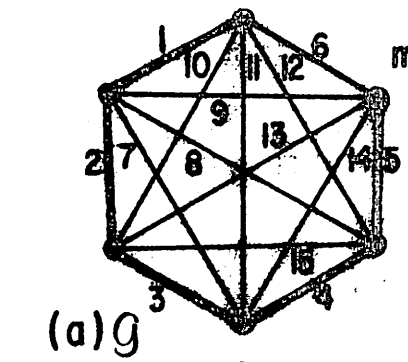

(a) $\mathcal{G}$

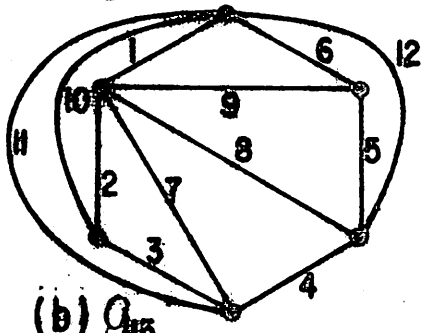

(b) $\mathcal{G}_{15}$

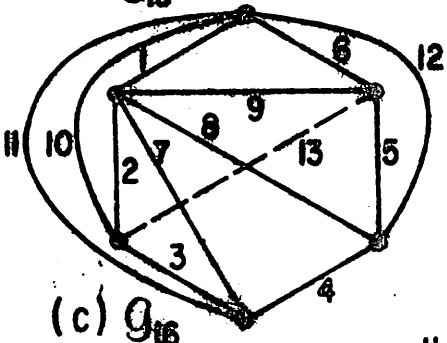

(c) $\mathcal{G}_{16}$

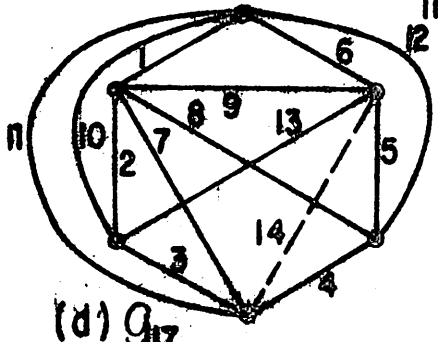

(d) $\mathcal{G}_{17}$

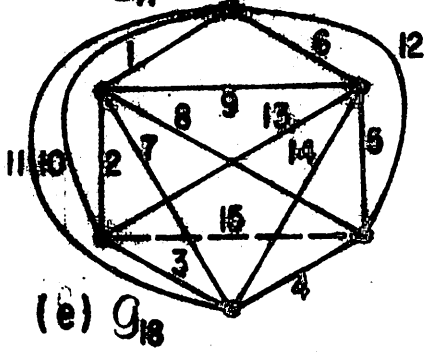

(e) $\mathcal{G}_{18}$

branch / mesh

X	X							X							4
		X					X	X							3
			X			X	X								1
				X	X	X									4
				X					X	X					3
X					X				X						2
	X	X									X				1
					X			X				X			1
				X								X	X		0
									X		X			X	Σ=19
2	2	2	1	2	2	2	2	2	2	1	1	0	0	0	$CL(M_0)$
2	2	2	1	2	3	2	2	3	2	1	1	1	0	0	$CL(M_1)$
2	2	2	1	3	3	2	2	3	2	1	1	2	1	0	$CL(M_2)$
2	2	2	1	3	3	2	2	3	3	1	2	2	1	1	$CL(M_3)$

(f) $\hat{\underset{\sim}{M}}$

branch / link

X	X	X	X	X	X										9
X	X	X	X			X									8
X	X	X					X								6
X	X							X							3
	X	X	X	X					X						5
	X	X	X							X					4
	X	X									X				2
		X	X	X								X			2
		X	X										X		1
			X	X										X	Σ=40

(g) $\underset{\sim}{B}$

Fig. 7

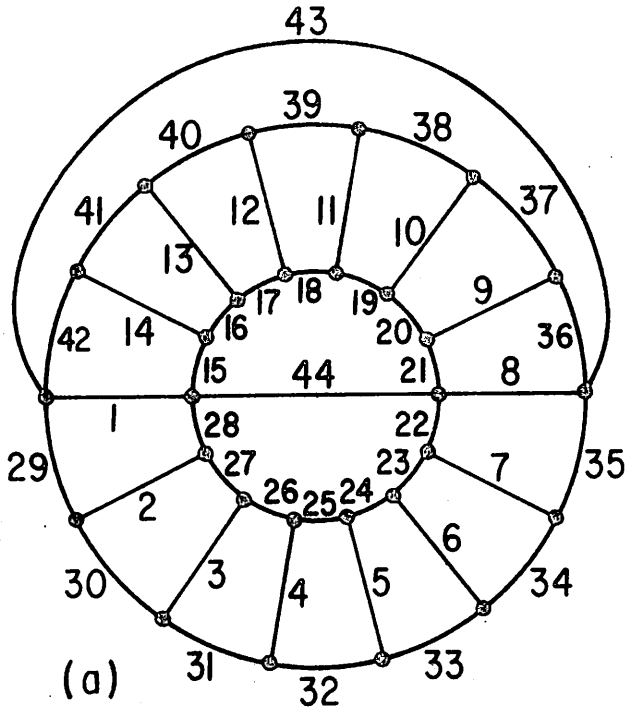

(a)

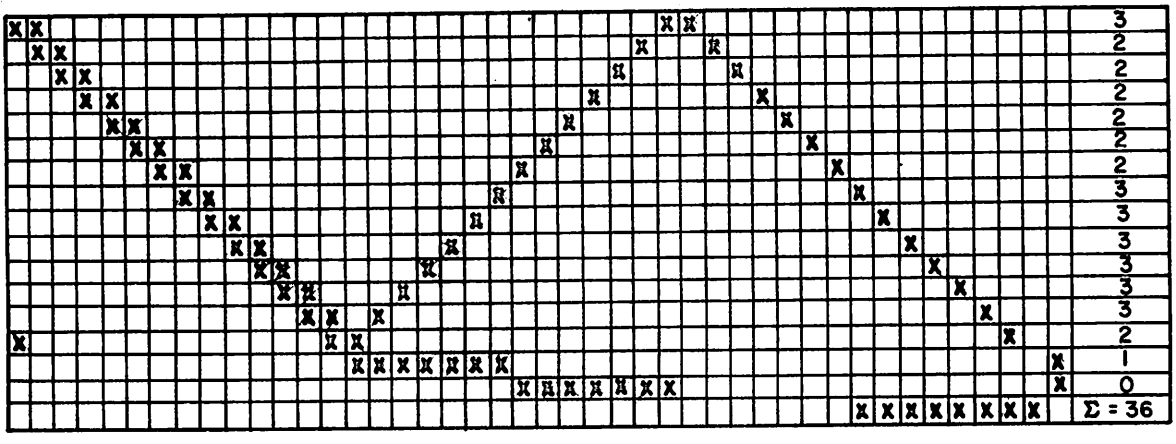

(b) $\underset{\sim}{M}$

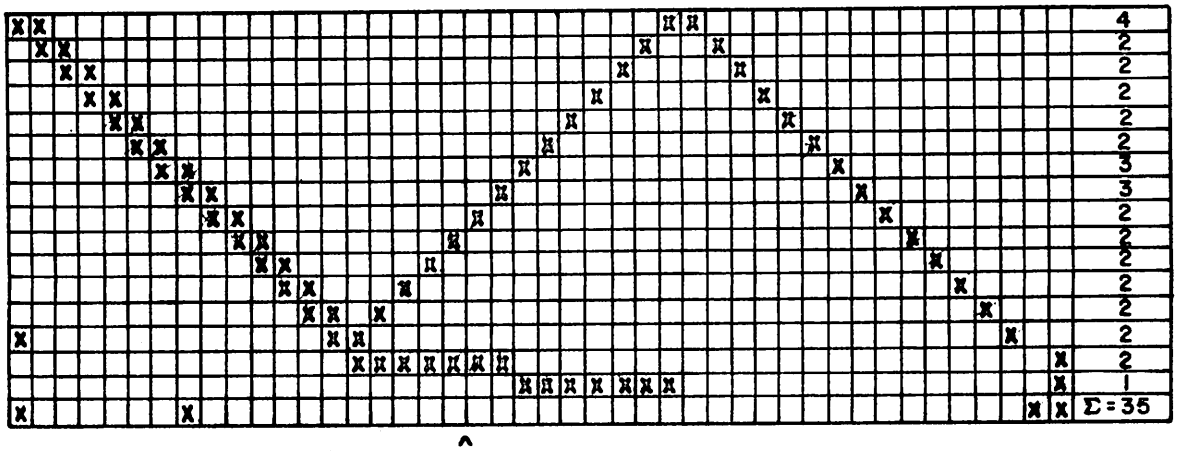

(c) $\underset{\sim}{\hat{B}}$

Fig. A-1

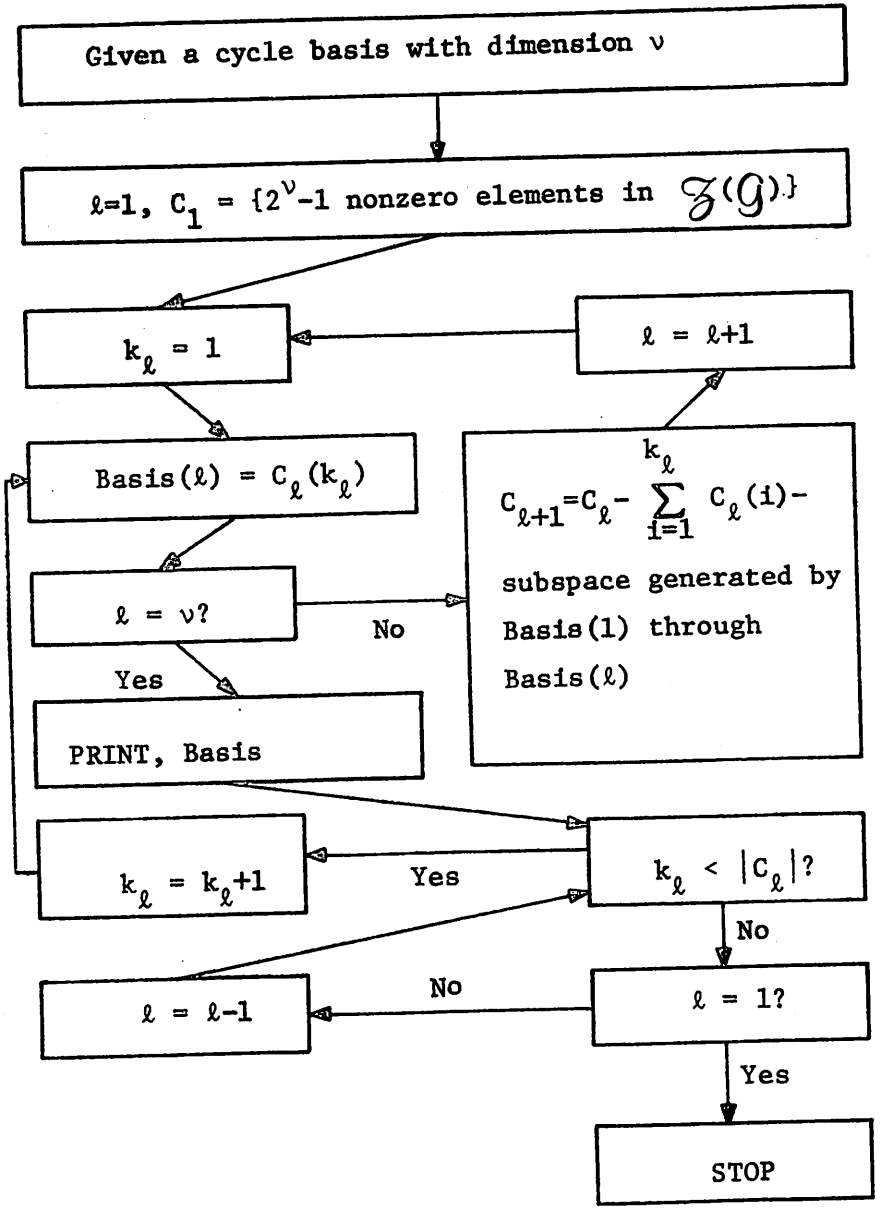

(a) Enumerating all basis

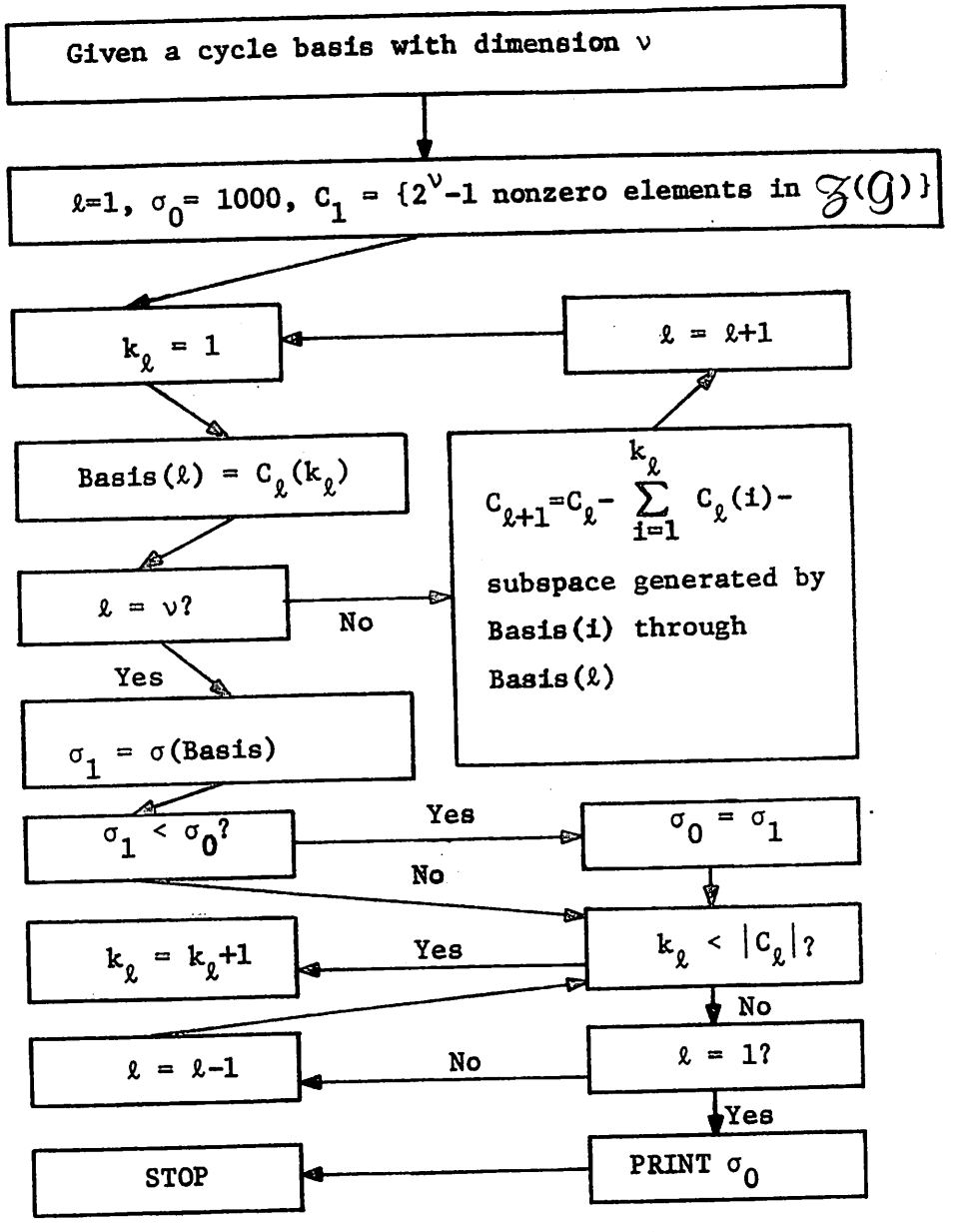

(b) Find σ_{opt}

Fig. A-2